Grand-potential formulation for multicomponent phase transformations combined with thin-interface asymptotics of the double-obstacle potential

Abhik Choudhury[*] and Britta Nestler[†]

Karlsruhe Institute of Technology (KIT), IAM-ZBS, Haid-und-Neu-Str. 7, D-76131 Karlsruhe, Germany

In this paper, we describe the derivation of a model for the simulation of phase transformations in multicomponent real alloys starting from a grand-potential functional. We first point out the limitations of a phase-field model when evolution equations for the concentration and the phase-field variables are derived from a free energy functional. These limitations are mainly attributed to the contribution of the grand-chemical-potential excess to the interface energy. For a range of applications, the magnitude of this excess becomes large and its influence on interface profiles and dynamics is not negligible. The related constraint regarding the choice of the interface thickness limits the size of the domain that can be simulated and, hence, the effect of larger scales on microstructure evolution can not be observed. We propose a modification to the model in order to decouple the bulk and interface contributions. Following this, we perform the thin-interface asymptotic analysis of the phase-field model. Through this, we determine the thin-interface kinetic coefficient and the antitrapping current to remove the chemical potential jump at the interface. We limit our analysis to the Stefan condition at lowest order in ϵ (parameter related to the interface width) and apply results from previous literature that the corrections to the Stefan condition (surface diffusion and interface stretching) at higher orders are removed when antisymmetric interpolation functions are used for interpolating the grand-potential densities and the diffusion mobilities.

I. INTRODUCTION AND MODEL MODIFICATION

Phase-field modeling has been used for alloy solidification and for the simulation of microstructures for more than a decade and the principal concepts are fairly well known, with the first ideas originating more than a century ago from the first works by Van der Waals, who proposed the use of a diffuse interface for treating capillary driven problems [1]. However, it is necessary to highlight the importance of certain modifications without which large scale quantitative microstructure simulations of the order of micrometers are not possible. In this paper, we describe a modification of the multi-phase-field model described in [2]. The foundation of this particular model is the entropy functional written as

$$\mathcal{S}(e,\boldsymbol{c},\boldsymbol{\phi}) = \int_{\Omega}\left[s(e,\boldsymbol{c},\boldsymbol{\phi}) - \left(\epsilon\tilde{a}(\boldsymbol{\phi},\nabla\boldsymbol{\phi}) + \frac{1}{\epsilon}\tilde{w}(\boldsymbol{\phi})\right)\right]d\Omega, \tag{1}$$

where e is the internal energy of the system, s is the bulk entropy density, and $\tilde{w}$ is the surface potential of the system. $\boldsymbol{c} = (c_1,\ldots,c_K)$ is the vector with the compositions of the K components and $\boldsymbol{\phi} = (\phi_1,\ldots,\phi_N)$ are the volume fractions of the N phases in the system. An equivalent form can be defined as a free energy functional at a given temperature T:

$$\mathcal{F}(T,\boldsymbol{c},\boldsymbol{\phi}) = \int_{\Omega}\left[f(T,\boldsymbol{c},\boldsymbol{\phi}) + \left(\epsilon a(\boldsymbol{\phi},\nabla\boldsymbol{\phi}) + \frac{1}{\epsilon}w(\boldsymbol{\phi})\right)\right]d\Omega. \tag{2}$$

The uniqueness lies in the usage of the double-obstacle potential $w(\boldsymbol{\phi}) = \{\sum_{\alpha<\beta}^{N,N}\gamma_{\alpha\beta}\frac{16}{\pi^2}\phi_\alpha\phi_\beta$, when $(\phi_\alpha,\phi_\beta > 0$ and $\phi_\alpha + \phi_\beta = 1)$ and ∞ elsewhere$\}$ in describing the surface

energy potential. However, if the free energies are interpolated as in [2,3], $f = \sum_{\alpha=1}^{N}f_\alpha(T,\boldsymbol{c},\boldsymbol{\phi})h_\alpha(\boldsymbol{\phi})$, where $f_\alpha(T,\boldsymbol{c})$ is the bulk free energy density of phase α and $h_\alpha(\boldsymbol{\phi})$ is an interpolation function for the phase α, two problems exist: (i) The surface energy $\sigma_{\alpha\beta}$ of an $\alpha\beta$ interface is a function of the chemical free energy density landscape in the system, and (ii) the equilibrium interface width $\Lambda_{\alpha\beta}$ becomes far too restrictive for simulating large scale microstructures.

These restrictions of the model will be highlighted in more detail in the following discussion. The equilibrium equation in one dimension (1D) for two phases α and β, where $\phi_\alpha + \phi_\beta = 1$, starting from the interpolation of the free energies can be written as

$$\gamma_{\alpha\beta}\epsilon\frac{\partial^2\phi_\alpha}{\partial x^2} = -\frac{16}{\pi^2}\frac{\gamma_{\alpha\beta}}{2\epsilon}(1-2\phi_\alpha) - \frac{1}{2}\frac{df}{d\phi_\alpha} + \frac{1}{2}\sum_{i=1}^{K-1}\mu_i\frac{dc_i}{d\phi_\alpha}$$

$$= -\frac{16}{\pi^2}\frac{\gamma_{\alpha\beta}}{2\epsilon}(1-2\phi_\alpha) - \frac{1}{2}\frac{d}{d\phi_\alpha}\left(f - \sum_{i=1}^{K-1}\mu_i c_i\right), \tag{3}$$

where $\boldsymbol{\mu} = (\mu_i,\ldots,\mu_{K-1})$ is the vector consisting of the $K-1$ equilibrium chemical potentials of the system at the given system temperature. Equation (3) can be used to derive the stationary solution of the phase field ϕ_α, which can be used to derive expressions for the surface energy of a binary interface $\sigma_{\alpha\beta}$ and equilibrium interface width $\Lambda_{\alpha\beta}$ as [4,5]

$$\sigma_{\alpha\beta}$$

$$= 2\gamma_{\alpha\beta}\int_0^1\sqrt{\left(\frac{16}{\pi^2}\phi_\alpha(1-\phi_\alpha) + \frac{\epsilon}{\gamma_{\alpha\beta}}[\Delta\Psi(T,\boldsymbol{c},\phi_\alpha)]\right)}d\phi_\alpha, \tag{4}$$

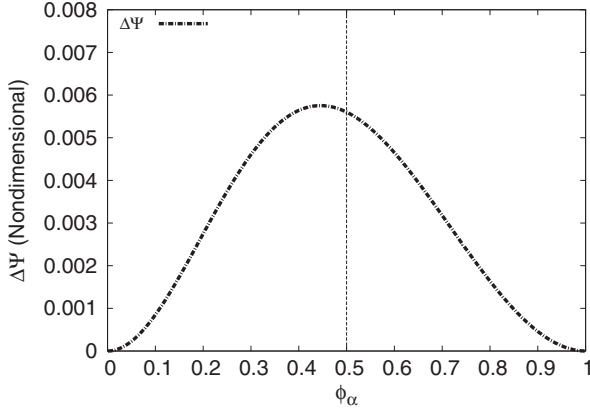[*]abhiknc@gmail.com
[†]britta.nestler@kit.edu

FIG. 1. The grand-chemical-potential difference varies across the interface and has a form similar to that of a potential. At equilibrium, the two phases are at the same grand chemical potential, which is seen qualitatively from the graph. Notice also the asymmetry of the potential around $\phi_\alpha = 0.5$, which is inherited from the asymmetry in the chemical free energy states of the two phases.

$$\Lambda_{\alpha\beta} = \epsilon \int_0^1 \frac{d\phi_\alpha}{\sqrt{\left(\frac{16}{\pi^2}\phi_\alpha(1-\phi_\alpha) + \frac{\epsilon}{\gamma_{\alpha\beta}}[\Delta\Psi(T,\boldsymbol{c},\phi_\alpha)]\right)}}. \quad (5)$$

Here, $\gamma_{\alpha\beta}$ is a term in the surface energy density, ϵ is a factor related to the length scale of the interface, and $\Delta\Psi(T,\boldsymbol{c},\phi_\alpha) = (f - \sum_{i=1}^{K-1}\mu_i c_i) - (f - \sum_{i=1}^{K-1}\mu_i c_i)_{\phi_\alpha=0}$ is the grand-chemical-potential difference between values at the interface and that of the bulk phases in equilibrium. At equilibrium, the terms $(f - \sum_{i=1}^{K-1}\mu_i c_i)_{\phi_\alpha=0}$ and $(f - \sum_{i=1}^{K-1}\mu_i c_i)_{\phi_\alpha=1}$ are equal, and Fig. 1 plots the variation of the term $\Delta\Psi(T,\boldsymbol{c},\phi_\alpha)$. We clearly see that the term $\frac{1}{2}\frac{d}{d\phi_\alpha}(f - \sum_{i=1}^{K-1}\mu_i c_i)$ is nonzero across the interface.

The area under the curve is the grand-chemical-potential excess at the interface. This contribution affects the equilibrium shape and properties of the interface. From the above, the following is evident:

(i) The parameters $\sigma_{\alpha\beta}$ and $\Lambda_{\alpha\beta}$ can not be fixed independently of the grand-chemical-potential contribution in the form $\Delta\Psi(T,\boldsymbol{c},\phi_\alpha)$.

(ii) Given the required $\sigma_{\alpha\beta}$ and $\Lambda_{\alpha\beta}$, the simulation parameters $\gamma_{\alpha\beta}$ and ϵ can be determined by simultaneously solving Eqs. (4) and (5). Notice that even though we have one parameter ϵ, the resulting interface thicknesses can be different, depending on the excess $\Delta\Psi(T,\boldsymbol{c},\phi_\alpha)$.

For very large chemical excess contributions in the form of $\Delta\Psi(T,\boldsymbol{c},\phi_\alpha)$, Eqs. (4) and (5) can be written approximately as

$$\sigma_{\alpha\beta} = 2\sqrt{\gamma_{\alpha\beta}\epsilon} \int_0^1 \sqrt{[\Delta\Psi(T,\boldsymbol{c},\phi_\alpha)]}d\phi_\alpha \quad (6)$$

$$\Lambda_{\alpha\beta} = \sqrt{\gamma_{\alpha\beta}\epsilon} \int_0^1 \frac{d\phi_\alpha}{\sqrt{[\Delta\Psi(T,\boldsymbol{c},\phi_\alpha)]}}. \quad (7)$$

In this case, $\sigma_{\alpha\beta}$ and $\Lambda_{\alpha\beta}$ are no longer independent. The term $\frac{\sigma_{\alpha\beta}}{\Lambda_{\alpha\beta}}$ becomes just a function of the chemical free energy of the system and independent of the terms $\gamma_{\alpha\beta}$ and ϵ.

This implies that once a value for $\sigma_{\alpha\beta}$ is chosen, the value of $\Lambda_{\alpha\beta}$ is fixed, and for certain choices of $\sigma_{\alpha\beta}$, the $\Lambda_{\alpha\beta}$ gets prohibitively lower, which makes simulation of larger domain structures unfeasible. These relationships have been studied fairly extensively in the past decade, and two principal solutions have been suggested [4,6–8]. The ideology is to completely avoid any contribution of the grand-chemical-potential excess contribution to the interface excess. This implies that the stationary solution is independent of any chemical contribution. While this is achieved in the work by [4,7,8] through the use of different concentration fields c_i^α in each phase, the same is affected for dilute alloys, with a single concentration field but the use of effective interpolation functions to interpolate the entropy and enthalpy contributions to the free energy. The common idea is that the driving force for phase transformation is the grand-potential difference between the phases at the same chemical potential. We motivate a similar idea from the following discussion.

A. Motivation

Consider the phase-field evolution equation in 1D at the lowest order in ϵ, which is a parameter related to the interface thickness:

$$\omega\epsilon\frac{\partial\phi_\alpha}{\partial t} = \gamma_{\alpha\beta}\epsilon\frac{\partial^2\phi_\alpha}{\partial x^2} - \frac{16}{\pi^2}\frac{\gamma_{\alpha\beta}}{2\epsilon}(1-2\phi_\alpha)$$
$$- \frac{1}{2}\frac{d}{d\phi_\alpha}\left(f - \sum_{i=1}^{K-1}\mu_i c_i\right), \quad (8)$$

where ω is the relaxation constant of the interface. This is also the evolution equation at the *sharp-interface limit* for this model [9]. The chemical potential $\boldsymbol{\mu} = (\mu_1,\dots,\mu_{K-1})$ is constant across the interface in this limit. For small velocities, the evolution equation in moving coordinate frame in 1D, at steady state velocity V, reads as

$$-V\tau\epsilon\frac{d\phi_\alpha}{dx} = \gamma_{\alpha\beta}\epsilon\frac{d^2\phi_\alpha}{dx^2} - \frac{16}{\pi^2}\frac{\gamma_{\alpha\beta}}{2\epsilon}(1-2\phi_\alpha)$$
$$- \frac{1}{2}\frac{d}{d\phi_\alpha}\left(f - \sum_{i=1}^{K-1}\mu_i c_i\right). \quad (9)$$

It is important to note that the moving frame is moving with velocity V along with the interface, which is denoted by the contour line $\phi_\alpha = 0.5$. By multiplying with $\frac{d\phi_\alpha}{dx}$ on both sides and integrating, we get

$$-V\tau\epsilon\int_{-\infty}^{\infty}\left(\frac{d\phi_\alpha}{dx}\right)^2 dx$$
$$= \int_{-\infty}^{\infty}\gamma_{\alpha\beta}\epsilon\frac{d^2\phi_\alpha}{dx^2}\frac{d\phi_\alpha}{dx}dx - \int_{-\infty}^{\infty}\frac{16}{\pi^2}\frac{\gamma_{\alpha\beta}}{2\epsilon}(1-2\phi_\alpha)\frac{d\phi_\alpha}{dx}dx$$
$$- \int_{-\infty}^{\infty}\frac{1}{2}\frac{d}{d\phi_\alpha}\left(f - \sum_{i=1}^{K-1}\mu_i c_i\right)\frac{d\phi_\alpha}{dx}dx.$$

We denote the integral $\int_{-\infty}^{\infty}(\frac{d\phi_\alpha}{dx})^2 dx$ as (I) and elaborate the other integrals as follows:

$$-V\tau\epsilon\text{I} = \frac{\gamma_{\alpha\beta}\epsilon}{2}\left(\frac{d\phi_\alpha}{dx}\right)^2\bigg|_{-\infty}^{\infty} - \frac{16}{\pi^2}\frac{\gamma_{\alpha\beta}}{2\epsilon}\phi_\alpha(1-\phi_\alpha)\bigg|_0^1$$
$$- \frac{1}{2}\left(f - \sum_{i=1}^{K-1}\mu_i c_i\right)\bigg|_0^1. \quad (10)$$

The first two integrals on the right-hand side drop out to zero and so the velocity of the interface can be written as

$$-V\tau\epsilon\text{I} = \frac{1}{2}\left(f - \sum_{i=1}^{K-1}\mu_i c_i\right)\bigg|_0^1. \quad (11)$$

Clearly, the interface mobility is proportional to the difference of the *grand chemical potential* of the two phases. Adequately, the driving force for phase transformation in alloys in the sharp-interface limit is the difference of the grand potentials of the two bulk phases. The evolution equations drive the system in a direction to reduce the difference of grand potentials between the bulk phases. This being the case, the motivation arises to formulate the phase-field model in terms of a grand-potential functional for the case of alloys.

B. Model modification

We write the grand potential Ψ as an interpolation of the individual grand potentials Ψ_α, where Ψ_α are functions of the chemical potential $\boldsymbol{\mu}$ and temperature T in the system

$$\Psi(T,\boldsymbol{\mu},\boldsymbol{\phi}) = \sum_{\alpha=1}^{N}\Psi_\alpha(T,\boldsymbol{\mu})h_\alpha(\boldsymbol{\phi}) \quad \text{with} \quad (12)$$

$$\Psi_\alpha(T,\boldsymbol{\mu}) = f_\alpha(\boldsymbol{c}^\alpha(\boldsymbol{\mu},T),T) - \sum_{i=1}^{K-1}\mu_i c_i^\alpha(\boldsymbol{\mu},T). \quad (13)$$

The concentration $c_i^\alpha(\boldsymbol{\mu},T)$ is an inverse of the function $\mu_i^\alpha(\boldsymbol{c},T)$ for every phase α and component i. From Eq. (13), the following relation can be derived:

$$\frac{\partial\Psi(T,\boldsymbol{\mu},\boldsymbol{\phi})}{\partial\mu_i} = \sum_{\alpha=1}^{N}\frac{\partial\Psi_\alpha(T,\boldsymbol{\mu})}{\partial\mu_i}h_\alpha(\boldsymbol{\phi}). \quad (14)$$

Since the grand chemical potential $\Psi(T,\boldsymbol{\mu},\boldsymbol{\phi})$ is the *Legendre transform* of the free energy density of the system $f(T,\boldsymbol{c},\boldsymbol{\phi})$, and from their coupled relation $\frac{\partial\Psi(T,\boldsymbol{\mu},\boldsymbol{\phi})}{\partial\mu_i} = -c_i$, it follows that

$$c_i = \sum_{\alpha=1}^{N}c_i^\alpha(\boldsymbol{\mu},T)h_\alpha(\boldsymbol{\phi}). \quad (15)$$

The above is the constraint used in [4,7,8] to determine the concentrations c_i^α in the interface along with the condition that the phase concentrations c_i^α are related by the condition of common equilibrium chemical potential among all the phases. This, however, derives elegantly starting from the grand chemical potential. It is important to note that the entire structure rests on the invertibility of the function $\mu^\alpha(\boldsymbol{c},T)$. This would result in a unique grand potential for a given $\boldsymbol{\mu}$.
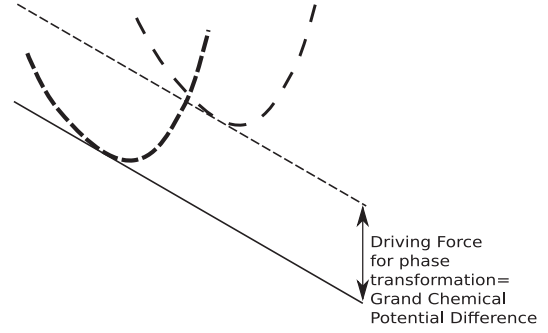

FIG. 2. Illustration of the driving force for phase transformation between two phases.

Since at equilibrium the grand chemical potentials of the phases are equal, for a two phase interface we can write

$$\Psi(T,\boldsymbol{\mu}_{eq}) = \Psi_\alpha(T,\boldsymbol{\mu}_{eq}) = \Psi_\beta(T,\boldsymbol{\mu}_{eq}). \quad (16)$$

This implies that at equilibrium the surface energy has no contribution from the chemical free energy and, equivalently, the chemical-grand-potential excess $\Delta\Psi$ is zero. The consequence of this is that the surface energy $\sigma_{\alpha\beta}$ is the same as the simulation parameter $\gamma_{\alpha\beta}$. Also, it can be derived that the equilibrium interface width $\Lambda_{\alpha\beta}$ is independent of the chemical free energy of the system and is related to constant ϵ by the relation $\frac{\pi^2}{4}\epsilon$ for the obstacle potential. The grand-chemical-potential difference can be visualized as in Fig. 2. A corollary of the above discussion is that the free energy of a mixture of two phases for alloys is not the interpolation of the free energies of the respective phases at a given concentration, but it is a mixture of the phases at the respective concentrations at which they are at thermodynamic equilibrium, i.e., at the same chemical potential $\boldsymbol{\mu}$. This can be realized through the reverse Legendre transform of the expression in Eq. (13), which gives

$$f(T,\boldsymbol{c},\boldsymbol{\phi}) = \sum_{\alpha=1}^{N}f_\alpha(\boldsymbol{c}^\alpha(\boldsymbol{\mu},T),T)h_\alpha(\phi_\alpha). \quad (17)$$

This is the start point of the derivation of the KKS (Kim-Kim-Suzuki) model [4]. In summary, the principal result is that we write the evolution equations using the chemical potential $\boldsymbol{\mu}$, which is analogous to T for the case of pure materials. The driving force, which is the difference of free energies in the case of pure materials, translates to the difference of grand potentials for alloys.

Note: Strictly speaking, the grand potential is defined in terms of the number of particles of the various components written as $G - \sum_{i=1}^{K-1}\mu_i N_i$, where G is the free energy of the system of N particles, and N_i is the number of particles of component i, while $\mu_i = \frac{\partial G}{\partial N_i}$. In the discussion on phase field, we require the energy densities of the respective phases, and hence, the energy of the system is generally divided by the volume of the system, which for the case of 1 mole of particles would be V_m, which is the molar volume. Also, the number of particles can be written in terms of the concentrations "mole fraction" through the relation $N_i = c_i N_o$, where N_o is the Avogadro number. By utilizing this, it is easy to see that $N_i\frac{\partial G}{\partial N_i} = V_m c_i\frac{\partial f}{\partial c_i}$, where $G = fV_m$ and we have assumed the

molar volumes of all particles the same. This implies that the total grand potential can be written as $V_m(f - \sum_{i=1}^{K-1} \mu_i c_i)$, giving us the grand-potential density as $(f - \sum_{i=1}^{K-1} \mu_i c_i)$. This is the form, which is used in the entire paper.

C. Evolution equations

The evolution equations for the phase and concentration fields can be evaluated in the standard way. Phase evolution is determined by the phenomenological minimization of the modified functional, which is formulated as the *grand-potential functional*

$$
\Omega(T, \boldsymbol{\mu}, \boldsymbol{\phi})
$$
$$
= \int_{\Omega} \left[\Psi(T, \boldsymbol{\mu}, \boldsymbol{\phi}) + \left(\epsilon a(\boldsymbol{\phi}, \nabla\boldsymbol{\phi}) + \frac{1}{\epsilon} w(\boldsymbol{\phi}) \right) \right] d\Omega.
\tag{18}
$$

The concentration fields are obtained by a mass conservation equation for each of the $K - 1$ independent concentration variables c_i. The evolution equation for the N phase-field variables can be written as

$$
\omega\epsilon \frac{\partial \phi_\alpha}{\partial t} = \epsilon \left(\nabla \cdot \frac{\partial a(\boldsymbol{\phi}, \nabla\boldsymbol{\phi})}{\partial \nabla\phi_\alpha} - \frac{\partial a(\boldsymbol{\phi}, \nabla\boldsymbol{\phi})}{\partial \phi_\alpha} \right)
$$
$$
- \frac{1}{\epsilon} \frac{\partial w(\boldsymbol{\phi})}{\partial \phi_\alpha} - \frac{\partial \Psi(T, \boldsymbol{\mu}, \boldsymbol{\phi})}{\partial \phi_\alpha} - \lambda,
\tag{19}
$$

where λ is the Lagrange parameter to maintain the constraint $\sum_{\alpha=1}^{N} \phi_\alpha = 1$. $a(\boldsymbol{\phi}, \nabla\boldsymbol{\phi})$ represents the gradient energy density and has the form

$$
a(\boldsymbol{\phi}, \nabla\boldsymbol{\phi}) = \sum_{\substack{\alpha,\beta = 1 \\ (\alpha < \beta)}}^{N,N} \gamma_{\alpha\beta} [a_c(q_{\alpha\beta})]^2 |q_{\alpha\beta}|^2,
\tag{20}
$$

where $q_{\alpha\beta} = (\phi_\alpha \nabla\phi_\beta - \phi_\beta \nabla\phi_\alpha)$ is a normal vector to the $\alpha\beta$ interface. $a_c(q_{\alpha\beta})$ describes the form of the anisotropy of the evolving phase boundary. The double-obstacle potential $w(\boldsymbol{\phi})$, which was also previously described in [2,3], can be written as

$$
w(\boldsymbol{\phi}) = \frac{16}{\pi^2} \sum_{\substack{\alpha,\beta = 1 \\ (\alpha < \beta)}}^{N,N} \gamma_{\alpha\beta} \phi_\alpha \phi_\beta,
\tag{21}
$$

where $\gamma_{\alpha\beta}$ is the surface energy density. The evolution equation for the concentration fields can be derived as

$$
\frac{\partial c_i}{\partial t} = \nabla \cdot \left(\sum_{j=1}^{K-1} M_{ij}(\boldsymbol{\phi}) \nabla\mu_j \right).
\tag{22}
$$

Here, $M_{ij}(\boldsymbol{\phi})$ is the mobility of the interface, where the individual phase mobilities are interpolated as

$$
M_{ij}(\boldsymbol{\phi}) = \sum_{\alpha=1}^{N-1} M_{ij}^\alpha g_\alpha(\boldsymbol{\phi}),
\tag{23}
$$

where each of the M_{ij}^α is defined using the expression

$$
M_{ij}^\alpha = D_{ij}^\alpha \frac{\partial c_i^\alpha(\boldsymbol{\mu}, T)}{\partial \mu_j}.
\tag{24}
$$

The function $g_\alpha(\boldsymbol{\phi})$ interpolates the mobilities and is in general not the same as $h_\alpha(\boldsymbol{\phi})$, which interpolates the grand potentials. D_{ij}^α are the interdiffusivities in each phase α. Both the evolution equations require the information about the chemical potential $\boldsymbol{\mu}$. Two possibilities exist to determine the unknown chemical potential $\boldsymbol{\mu}$:

(i) The chemical potential $\boldsymbol{\mu}$ can be derived from the constraint relation (15). The $K - 1$ independent components μ_i are determined by simultaneously solving the $K - 1$ constraints for each of the $K - 1$ independent concentration variables c_i, from the given values of c_i and ϕ_α at a given grid point. A Newton iteration scheme can be used for solving the system of equations

$$
\{\mu_i^{n+1}\} = \{\mu_i^n\} - \left[\sum_{\alpha=1}^{N} h_\alpha(\boldsymbol{\phi}) \frac{\partial c_i^\alpha(\boldsymbol{\mu}^n, T)}{\partial \mu_j} \right]_{ij}^{-1}
$$
$$
\times \left\{ c_i - \sum_{\alpha=1}^{N} c_i^\alpha(\boldsymbol{\mu}^n, T) h_\alpha(\boldsymbol{\phi}) \right\}.
\tag{25}
$$

This is precisely the approach in the KKS model [4]. However, there is a substantial difference in that we propose to solve directly for the thermodynamic variable $\boldsymbol{\mu}$, which relate the phase concentrations c_i^α instead of solving for phase concentrations themselves. This is possible because the concentrations $c_i^\alpha(\boldsymbol{\mu}, T)$ are written as explicit functions of the thermodynamic variable $\boldsymbol{\mu}$. The method also bears similarity to the method of [7,8], where a partition relation is used to close the relationship between the phase concentrations.

(ii) Alternatively, explicit evolution equations for all the $K - 1$ independent chemical potentials can be formulated by inserting the constraint equation (15) into the evolution equation for the concentration field, Eq. (22). For a two phase binary alloy, i.e., $(\phi_\alpha + \phi_\beta = 1)$ and $c_A + c_B = 1$, the evolution equation can be written as

$$
\left(\frac{\partial c^\alpha(\mu, T)}{\partial \mu} h_\alpha(\boldsymbol{\phi}) + \frac{\partial c^\beta(\mu, T)}{\partial \mu} [1 - h_\alpha(\boldsymbol{\phi})] \right) \frac{\partial \mu}{\partial t}
$$
$$
= \nabla \cdot \left[\left(D^\alpha g_\alpha(\boldsymbol{\phi}) \frac{\partial c^\alpha(\mu, T)}{\partial \mu} \right.\right.
$$
$$
\left.\left. + D^\beta [1 - g_\alpha(\boldsymbol{\phi})] \frac{\partial c^\beta(\mu, T)}{\partial \mu} \right) \nabla\mu \right]
$$
$$
- [c^\alpha(\mu, T) - c^\beta(\mu, T)] \frac{\partial h_\alpha(\boldsymbol{\phi})}{\partial t},
$$

where $c^{\alpha,\beta}(\mu)$ are the phase concentrations as functions of the independent chemical potential μ. D^α, D^β are the independent interdiffusivities in the two respective phases. It is noteworthy that this equation looks very similar to the evolution equation of the temperature field in pure materials. The last term on the right-hand side $c^\alpha(\mu, T) - c^\beta(\mu, T)$ corresponds to a source term for rejection of mass at the interface during growth, which is analogous to the release of latent heat in pure material solidification. For a general, multiphase, multicomponent system, the evolution equations for the components of the chemical potential $\boldsymbol{\mu}$ can be written in matrix form

by

$$\left\{ \frac{\partial \mu_i}{\partial t} \right\} = \left[\sum_{\alpha=1}^{N} h_\alpha(\boldsymbol{\phi}) \frac{\partial c_i^\alpha(\boldsymbol{\mu},T)}{\partial \mu_j} \right]_{ij}^{-1}$$

$$\times \left\{ \nabla \cdot \sum_{j=1}^{K-1} M_{ij}(\boldsymbol{\phi}) \nabla \mu_j - \sum_{\alpha}^{N} c_i^\alpha(\boldsymbol{\mu},T) \frac{\partial h_\alpha(\boldsymbol{\phi})}{\partial t} \right\}.$$
(26)

The above derivation bears a lot of resemblance to the recent derivation by Plapp [10]. It is worth to comment on how the two methods compare in the computational complexity. For this, it is first essential to identify the similarity of the approaches, as can be seen by comparing Eqs. (25) and (26). Consider the case when Eq. (25) is written for the case of binary alloy, which reads as

$$\mu^{n+1} = \mu^n + \frac{c - \sum_{\alpha=1}^{N} c^\alpha(\mu^n,T) h_\alpha(\boldsymbol{\phi})}{\sum_{\alpha=1}^{N} \frac{\partial c^\alpha(\mu^n,T)}{\partial \mu} h_\alpha(\boldsymbol{\phi})},$$
(27)

where we intend to calculate the μ for the next time step $(t+1)$, μ^n being the start guess for the iteration that satisfies the equation $c - \sum_{\alpha=1}^{N} c^\alpha(\mu^n,T) h_\alpha(\boldsymbol{\phi}) = 0$ for the values of $c = c^o$ and $\boldsymbol{\phi} = \boldsymbol{\phi}^o$ at the time step t. By expanding the second term on the right-hand side in En. (27) for small change in time δt, we can write

$$\mu^{n+1} - \mu^n = \frac{c^o - \sum_{\alpha=1}^{N} c^\alpha(\mu^n,T) h_\alpha(\boldsymbol{\phi}^o)}{\sum_{\alpha=1}^{N} \frac{\partial c^\alpha(\mu^n,T)}{\partial \mu} h_\alpha(\boldsymbol{\phi}^o)}$$
$$+ \delta t \left(\frac{\frac{\partial c}{\partial t} - \sum_{\alpha=1}^{N} c^\alpha(\mu^n,T) \frac{\partial h_\alpha(\boldsymbol{\phi}^o)}{\partial t}}{\sum_{\alpha=1}^{N} \frac{\partial c^\alpha(\mu^n,T)}{\partial \mu} h_\alpha(\boldsymbol{\phi}^o)} \right)$$
$$+ O(\delta t^2).$$
(28)

Note that additional terms arise out of the linear expansion, but we simplify using the fact that $c^0 - \sum_{\alpha=1}^{N} c^\alpha(\mu^n,T) h_\alpha(\boldsymbol{\phi}^0) = 0$. Using the same fact, the preceding equation simplifies to

$$\frac{\mu^{n+1} - \mu^n}{\delta t} = \left(\frac{\frac{\partial c}{\partial t} - \sum_{\alpha=1}^{N} c^\alpha(\mu^n,T) \frac{\partial h_\alpha(\boldsymbol{\phi}^o)}{\partial t}}{\sum_{\alpha=1}^{N} \frac{\partial c^\alpha(\mu^n,T)}{\partial \mu} h_\alpha(\boldsymbol{\phi}^o)} \right) + O(\delta t),$$
(29)

which in the region of small enough δt implies convergence is achieved in one iteration and hence can be written as

$$\frac{\partial \mu}{\partial t} = \left(\frac{\nabla \cdot (M \nabla \mu) - \sum_{\alpha=1}^{N} c^\alpha(\mu^n,T) \frac{\partial h_\alpha(\boldsymbol{\phi}^o)}{\partial t}}{\sum_{\alpha=1}^{N} \frac{\partial c^\alpha(\mu^n,T)}{\partial \mu} h_\alpha(\boldsymbol{\phi}^o)} \right).$$
(30)

The derived equation is identical to the binary variant of Eq. (26). It is not surprising to see the similarity since we are essentially solving for the same variable $\boldsymbol{\mu}$ and the difference is that while Eq. (25) is an implicit type of calculation scheme of the chemical potential, Eq. (26) describes an explicit computation. It would be interesting to compare the performance and accuracy of both methods.

II. ASYMPTOTIC ANALYSIS

In this section, we perform the asymptotic analysis of the phase-field model for a two phase binary alloy solidification with the assumption of one-sided diffusion in the liquid and vanishing diffusivity in the solid. Our aim is to derive the expressions for the kinetic coefficient in the thin-interface limit for the case of solute diffusion by performing an asymptotic analysis unto second order in the phase field, and for this purpose the analysis in 1D suffices. The asymptotic analysis is applied to the presented model ensuring no free energy excess at the interface. For simplicity, we treat here a two phase binary alloy. Hence, the chemical potential $\boldsymbol{\mu}$ will be written as μ since there exists only one independent chemical potential. At the onset, we express the grand potentials $\Psi_\alpha(\mu,T)$ as a linear expansion about the equilibrium chemical potential μ_{eq}:

$$\Psi_\alpha(T,\mu) = \Psi_\alpha(T,\mu_{eq}) + \left. \frac{\partial \Psi_\alpha(T,\mu)}{\partial \mu} \right|_{\mu_{eq}} (\mu - \mu_{eq}). \quad (31)$$

The driving force ΔF^α is then

$$\Delta F^\alpha = [\Psi_\alpha(T,\mu) - \Psi_\beta(T,\mu)] \frac{\partial h_\alpha(\boldsymbol{\phi})}{\partial \phi_\alpha} \quad (32)$$

$$= \left(\left. \frac{\partial \Psi_\alpha(T,\mu)}{\partial \mu} \right|_{\mu_{eq}} - \left. \frac{\partial \Psi_\beta(T,\mu)}{\partial \mu} \right|_{\mu_{eq}} \right)$$

$$\times (\mu - \mu_{eq}) \frac{\partial h_\alpha(\boldsymbol{\phi})}{\partial \phi_\alpha} \quad (33)$$

$$= -[c^\alpha(\mu_{eq},T) - c^\beta(\mu_{eq},T)](\mu - \mu_{eq}) \frac{\partial h_\alpha(\boldsymbol{\phi})}{\partial \phi_\alpha},$$
(34)

implying that the evolution equation for the phase field for a two phase system can be written as

$$\omega \epsilon^2 \frac{\partial \phi_\alpha}{\partial t} = \epsilon^2 \gamma_{\alpha\beta} \frac{\partial^2 \phi_\alpha}{\partial x^2} - \frac{16}{2\pi^2} \gamma_{\alpha\beta} (1 - 2\phi_\alpha)$$
$$+ \frac{1}{2} \epsilon [c^\alpha(\mu_{eq},T) - c^\beta(\mu_{eq},T)]$$
$$\times (\mu - \mu_{eq}) \frac{\partial h_\alpha(\phi_\alpha)}{\partial \phi_\alpha}. \quad (35)$$

Notice that we have reduced a system of two dependent equations to one independent equation by incorporating the Lagrange multiplier formalism. Also, the interpolation function $h_\alpha(\boldsymbol{\phi})$ is now for the two phase system just a function of ϕ_α. Hence, for the forthcoming derivations, we will omit the vector notation. The interpolation functions satisfy the property $h_\alpha(\phi_\alpha) = 1 - h_\beta(\phi_\beta)$. *Further, we consider small deviations from equilibrium, which is generally a suitable assumption for most cases of solidification. For larger driving forces, such as in rapid solidification, this assumption of the linearization of the driving forces will no longer hold.* For the case where we have $D^\alpha \ll D^\beta$, the evolution equation for the chemical potential of a binary system reads as

$$\left(\frac{\partial c^\alpha(\mu,T)}{\partial \mu} h_\alpha(\phi_\alpha) + \frac{\partial c^\beta(\mu,T)}{\partial \mu} [1 - h_\alpha(\phi_\alpha)] \right) \frac{\partial \mu}{\partial t}$$
$$= \nabla \cdot \left[\left(D^\beta [1 - g_\alpha(\phi_\alpha)] \frac{\partial c^\beta(\mu,T)}{\partial \mu} \right) \nabla \mu \right]$$
$$- [c^\alpha(\mu,T) - c^\beta(\mu,T)] \frac{\partial h_\alpha(\phi_\alpha)}{\partial t}. \quad (36)$$

We nondimensionalize the system of equations (35) and (36) by choosing the length scale $d_o = \frac{\gamma_{\alpha\beta}}{f^*}$, where f^* is the energy

scale of the system, the time scale $t* = \frac{d_0^2}{D_\beta}$ with D_β being the diffusivity in the liquid, and replace ω with nondimensionalized parameter ζ as $\frac{D\omega}{\gamma_{\alpha\beta}}$. The nondimensional phase-field equation yields with the described scaling parameters

$$\zeta\epsilon^2\frac{\partial\phi_\alpha}{\partial t} = \epsilon^2\frac{\partial^2\phi_\alpha}{\partial x^2} - \frac{16}{2\pi^2}(1-2\phi_\alpha)$$
$$+ \frac{1}{2}\epsilon[c^\alpha(\mu_{eq},T) - c^\beta(\mu_{eq},T)]$$
$$\times (\mu - \mu_{eq})\frac{\partial h_\alpha(\phi_\alpha)}{\partial\phi_\alpha}, \qquad (37)$$

while the nondimensionalized chemical potential equation can be written as

$$\left(\frac{\partial c^\alpha(\mu,T)}{\partial\mu}h_\alpha(\phi_\alpha) + \frac{\partial c^\beta(\mu,T)}{\partial\mu}[1-h_\alpha(\phi_\alpha)]\right)\frac{\partial\mu}{\partial t}$$
$$= \nabla\cdot\left([1-g_\alpha(\phi_\alpha)]\frac{\partial c^\beta(\mu,T)}{\partial\mu}\nabla\mu\right)$$
$$- [c^\alpha(\mu,T) - c^\beta(\mu,T)]\frac{\partial h_\alpha(\phi_\alpha)}{\partial t}. \qquad (38)$$

For our further analysis, we choose the chemical potential equation for the asymptotic expansions. For the case of one-sided diffusion, it has been shown in various previous works [11,12] that there exists a thin-interface defect called *solute trapping* when simulations are performed with interface thicknesses, orders of magnitude larger than those of a real interface. One must note that, although this is a phenomenon observed in experiments, the artifact in the phase-field simulations occurs at velocities much lower than those in the experiments where solute trapping is reported. The methodology proposed to correct this effect is the incorporation of an antitrapping current in the evolution equation of the chemical potential. While such expressions have been derived for *double well* type potentials [6,11,13], the case of the double-obstacle potential is untreated so far. We complete this gap by deriving the thin-interface limit of the model for a *double-obstacle potential* and formulating an expression of the antitrapping current j_{at}

for the case of one-sided diffusion. We follow the formulations described in literature and incorporate the antitrapping term as an additional flux of solute from the solid to the liquid in the normal direction to the interface. The modified evolution equation for the chemical potential along with the antitrapping term is

$$\left(\frac{\partial c^\alpha(\mu,T)}{\partial\mu}h_\alpha(\phi_\alpha) + \frac{\partial c^\beta(\mu,T)}{\partial\mu}[1-h_\alpha(\phi_\alpha)]\right)\frac{\partial\mu}{\partial t}$$
$$= \nabla\cdot\left([1-g_\alpha(\phi_\alpha)]\frac{\partial c^\beta(\mu,T)}{\partial\mu}\nabla\mu - j_{at}\right)$$
$$- [c^\alpha(\mu,T) - c^\beta(\mu,T)]\frac{\partial h_\alpha(\phi_\alpha)}{\partial t}. \qquad (39)$$

To make sure that the antitrapping current appears in the first-order correction to the chemical potential, we formulate the antitrapping current of the following form:

$$j_{at} = s(\phi_\alpha)\epsilon[c^\beta(\mu,T) - c^\alpha(\mu,T)]\frac{\partial\phi_\alpha}{\partial t}\frac{q_{\alpha\beta}}{|q_{\alpha\beta}|}, \qquad (40)$$

where $s(\phi_\alpha)$ is a function such that the chemical potential jump vanishes at the interface. $q_{\alpha\beta}$ is the normal vector to the interface, given as $(\phi_\alpha\nabla\phi_\beta - \phi_\beta\nabla\phi_\alpha)$. *To see this, use $\phi_\alpha = \phi_\beta$ for the case of a binary interface between the α and the β interfaces. Then, the vector $q_{\alpha\beta}$ reduces to $\phi_\alpha\nabla(\phi_\beta - \phi_\alpha)$. Since the gradient of the scalar field $(\phi_\beta - \phi_\alpha)$ is normal to any contour $(\phi_\beta - \phi_\alpha) = const$, we have $\nabla(\phi_\beta - \phi_\alpha)$ normal to the contour $(\phi_\beta - \phi_\alpha) = 0$, which defines the binary interface.*

For the case of only two phases, it can be shown that the expression of the antitrapping current can be reduced to

$$j_{at} = -s(\phi_\alpha)\epsilon[c^\beta(\mu,T) - c^\alpha(\mu,T)]\frac{\partial\phi_\alpha}{\partial t}\frac{\nabla\phi_\alpha}{|\nabla\phi_\alpha|}. \qquad (41)$$

Note that all terms in the above equation are used in the nondimensional form, so ϵ is the nondimensional parameter related to the interface width and t is the nondimensional time. By writing the phase field and chemical potential evolution equations in one dimension, we have

$$\zeta\epsilon^2\frac{\partial\phi_\alpha}{\partial t} = \epsilon^2\frac{\partial^2\phi_\alpha}{\partial x^2} - \frac{16}{2\pi^2}(1-2\phi_\alpha) + \frac{1}{2}\epsilon[c^\alpha(\mu_{eq},T) - c^\beta(\mu_{eq},T)](\mu - \mu_{eq})\frac{\partial h_\alpha(\phi_\alpha)}{\partial\phi_\alpha}, \qquad (42)$$

$$\left(\frac{\partial c^\alpha(\mu,T)}{\partial\mu}h_\alpha(\phi_\alpha) + \frac{\partial c^\beta(\mu,T)}{\partial\mu}[1-h_\alpha(\phi_\alpha)]\right)\frac{\partial\mu}{\partial t}$$
$$= \frac{\partial}{\partial x}\left([1-g_\alpha(\phi_\alpha)]\frac{\partial c^\beta(\mu,T)}{\partial\mu}\frac{\partial\mu}{\partial x} - s(\phi_\alpha)\epsilon[c^\beta(\mu,T) - c^\alpha(\mu,T)]\frac{\partial\phi_\alpha}{\partial t}\right) - [c^\alpha(\mu,T) - c^\beta(\mu,T)]\frac{\partial h_\alpha(\phi_\alpha)}{\partial t}, \qquad (43)$$

which on transformation to the moving frame (fixed to $\phi_\alpha = 0.5$) becomes

$$-\zeta v\epsilon^2\frac{\partial\phi_\alpha}{\partial x} = \epsilon^2\frac{\partial^2\phi_\alpha}{\partial x^2} - \frac{16}{2\pi^2}(1-2\phi_\alpha) + \frac{1}{2}\epsilon[c^\alpha(\mu_{eq},T) - c^\beta(\mu_{eq},T)](\mu - \mu_{eq})\frac{\partial h_\alpha(\phi_\alpha)}{\partial\phi_\alpha}, \qquad (44)$$

$$-\left(\frac{\partial c^\alpha(\mu,T)}{\partial\mu}h_\alpha(\phi_\alpha) + \frac{\partial c^\beta(\mu,T)}{\partial\mu}[1-h_\alpha(\phi_\alpha)]\right)v\frac{\partial\mu}{\partial x}$$
$$= \frac{\partial}{\partial x}\left([1-g_\alpha(\phi_\alpha)]\frac{\partial c^\beta(\mu,T)}{\partial\mu}\frac{\partial\mu}{\partial x} + vs(\phi_\alpha)\epsilon[c^\beta(\mu,T) - c^\alpha(\mu,T)]\frac{\partial\phi_\alpha}{\partial x}\right) + v[c^\alpha(\mu,T) - c^\beta(\mu,T)]\frac{\partial h_\alpha(\phi_\alpha)}{\partial x}, \qquad (45)$$

where v is the nondimensional velocity scaled as $\frac{Vd_0}{D^\beta}$. To perform the asymptotic analysis, the region of evolution is divided into three parts. The "inner" region where there is rapid variation of the phase field ϕ_α and chemical potential μ, and two "outer"

regions, which denote regions where there is little change in the phase field ϕ_α. To probe into the inner solutions, we scale the coordinate with the parameter ϵ by introducing a scaling parameter $\eta = \frac{x}{\epsilon}$. With this scaling, the equations rewrite to

$$-\zeta v \epsilon \frac{\partial \phi_\alpha}{\partial \eta} = \frac{\partial^2 \phi_\alpha}{\partial \eta^2} - \frac{16}{2\pi^2}(1 - 2\phi_\alpha) + \frac{1}{2}\epsilon[c^\alpha(\mu_{eq},T) - c^\beta(\mu_{eq},T)](\mu - \mu_{eq})\frac{\partial h_\alpha(\phi_\alpha)}{\partial \phi_\alpha}, \tag{46}$$

$$-\left(\frac{\partial c^\alpha(\mu,T)}{\partial \mu}h_\alpha(\phi_\alpha) + \frac{\partial c^\beta(\mu,T)}{\partial \mu}[1 - h_\alpha(\phi_\alpha)]\right)\frac{v}{\epsilon}\frac{\partial \mu}{\partial \eta}$$

$$= \frac{1}{\epsilon^2}\frac{\partial}{\partial \eta}\left([1 - g_\alpha(\phi_\alpha)]\frac{\partial c^\beta(\mu,T)}{\partial \mu}\frac{\partial \mu}{\partial \eta}\right) + \frac{1}{\epsilon}\frac{\partial}{\partial \eta}\left(vs(\phi_\alpha)[c^\beta(\mu,T) - c^\alpha(\mu,T)]\frac{\partial \phi_\alpha}{\partial \eta}\right)$$

$$+ \frac{v}{\epsilon}[c^\alpha(\mu,T) - c^\beta(\mu,T)]\frac{\partial h_\alpha(\phi_\alpha)}{\partial \eta}. \tag{47}$$

The strategy is to write each of the outer and inner solutions as powers of the scaling parameter ϵ and match the outer and inner solutions order by order. The outer solutions are denoted by $\widetilde{\mu}$ and $\widetilde{\phi}_\alpha$ and are expanded by $\widetilde{\phi}_\alpha = \widetilde{\phi}_\alpha^0 + \epsilon\widetilde{\phi}_\alpha^1 + \epsilon^2\widetilde{\phi}_\alpha^2$ and $\widetilde{\mu} = \widetilde{\mu}^0 + \epsilon\widetilde{\mu}^1 + \epsilon^2\widetilde{\mu}^2$. The inner solutions similarly write as $\phi_\alpha = \phi_\alpha^0 + \epsilon\phi_\alpha^1 + \epsilon^2\phi_\alpha^2$ and $\mu = \mu^0 + \epsilon\mu^1 + \epsilon^2\mu^2$. The matching conditions between the outer and the inner solutions can be written by expanding each of the outer functions $\widetilde{\mu^0}, \widetilde{\mu^1}, \widetilde{\mu^2}$ as an expansion around $x = 0$, i.e., $x = (0 + \eta\epsilon)$ and equating them to the corresponding values of the inner solution. So, all the derivatives are computed at the position $x = 0$, marking the interface at $\phi_\alpha = 0.5$:

$$\lim_{\eta \to \pm\infty} \mu^0 = \widetilde{\mu^0}|^\pm, \tag{48}$$

$$\lim_{\eta \to \pm\infty} \mu^1 = \lim_{\eta \to \pm\infty}\left(\widetilde{\mu^1}|^\pm + \eta\frac{\partial\widetilde{\mu^0}}{\partial x}\bigg|^\pm\right), \tag{49}$$

$$\lim_{\eta \to \pm\infty} \mu^2 = \lim_{\eta \to \pm\infty}\left(\widetilde{\mu^2}|^\pm + \eta\frac{\partial\widetilde{\mu^1}}{\partial x}\bigg|^\pm + \frac{\eta^2}{2}\frac{\partial^2\widetilde{\mu^0}}{\partial x^2}\bigg|^\pm\right) \tag{50}$$

and the derivative matching conditions

$$\lim_{\eta \to \pm\infty} \frac{\partial\mu^0}{\partial \eta} = 0, \tag{51}$$

$$\lim_{\eta \to \pm\infty} \frac{\partial\mu^1}{\partial \eta} = \frac{\partial\widetilde{\mu^0}}{\partial x}\bigg|^\pm, \tag{52}$$

$$\lim_{\eta \to \pm\infty} \frac{\partial\mu^2}{\partial \eta} = \lim_{\eta \to \pm\infty}\left(\frac{\partial\widetilde{\mu^1}}{\partial x} + \eta\frac{\partial^2\widetilde{\mu^0}}{\partial x^2}\right). \tag{53}$$

The matching conditions for the phase field are trivial, as the phase field is constant in the bulk on both sides. Hence, the outer solution in the phase field is nonzero only for the lowest order. Now, we solve the phase field and chemical potential equations order by order and derive the various boundary conditions for the chemical potential as solvability conditions.

A. Sharp-interface limit

The phase-field equation at zero order in ϵ reads as

$$\frac{\partial^2 \phi_\alpha^0}{\partial \eta^2} - \frac{16}{2\pi^2}(1 - 2\phi_\alpha^0) = 0. \tag{54}$$

Integrating yields $\frac{\partial\phi_\alpha^0}{\partial\eta} = -\frac{4}{\pi}\sqrt{\phi_\alpha^0(1 - \phi_\alpha^0)}$, where the sign results from the boundary conditions $\lim_{\eta \to +\infty} \phi_\alpha^0 = 0$ and

$\lim_{\eta \to -\infty} \phi_\alpha^0 = 1$. The lowest order chemical potential equation at order $1/\epsilon^2$ is

$$\frac{1}{\epsilon^2}\frac{\partial}{\partial \eta}\left([1 - g_\alpha(\phi_\alpha^0)]\frac{\partial c^\beta(\mu^0,T)}{\partial \mu}\frac{\partial \mu^0}{\partial \eta}\right) = 0. \tag{55}$$

Integrating the above equation once, we get

$$[1 - g_\alpha(\phi_\alpha^0)]\frac{\partial c^\beta(\mu^0,T)}{\partial \mu}\frac{\partial \mu^0}{\partial \eta} = A_1. \tag{56}$$

We observe $\lim_{\eta \to \infty} g_\alpha(\phi_\alpha^0) = 0$ and the factor $\frac{\partial c^\beta(\mu^0,T)}{\partial \mu}$ is nonzero. By using the matching condition in Eq. (51), we derive that A_1 is zero. By inserting $A_1 = 0$ into Eq. (56) and integrating once, we get

$$\mu^0 = \overline{\mu^0}. \tag{57}$$

$\overline{\mu^0}$ is an integration constant. To fix the value, we insert this constant in the phase-field equation at order ϵ that reads as

$$-\zeta v \frac{\partial \phi_\alpha^0}{\partial \eta} = \frac{\partial^2 \phi_\alpha^1}{\partial \eta^2} + \frac{16}{\pi^2}\phi_\alpha^1 + \frac{1}{2}[c^\alpha(\mu_{eq},T) - c^\beta(\mu_{eq},T)]$$

$$\times (\mu^0 - \mu_{eq})\frac{\partial h_\alpha(\phi_\alpha^0)}{\partial \phi_\alpha}. \tag{58}$$

For brevity, we determine the constant $(\mu^0 - \mu_{eq})$ from the solvability condition. It is useful to identify a useful operator, which derives from the phase-field equation at zeroth order as

$$\frac{\partial^2 \phi_\alpha^0}{\partial \eta^2} - \frac{16}{2\pi^2}(1 - 2\phi_\alpha^0) = 0. \tag{59}$$

By differentiating the above equation and rearranging, we get

$$\left(\frac{\partial^2}{\partial \eta^2} + \frac{16}{\pi^2}\right)\frac{\partial \phi_\alpha^0}{\partial \eta} = 0. \tag{60}$$

The term in the brackets $\frac{\partial^2}{\partial \eta^2} + \frac{16}{\pi^2}$ is a linear operator and we define this as L. Using this linear operator, the phase-field equation at order ϵ is

$$L\phi_\alpha^1 = -\zeta v \frac{\partial \phi_\alpha^0}{\partial \eta} - \frac{1}{2}[c^\alpha(\mu_{eq},T) - c^\beta(\mu_{eq},T)]$$

$$\times (\mu^0 - \mu_{eq})\frac{\partial h_\alpha(\phi_\alpha^0)}{\partial \phi_\alpha}. \tag{61}$$

From Eq. (60), we see that $\frac{\partial \phi_\alpha^0}{\partial \eta}$ is a homogeneous solution of the operator L, hence, the solvability condition for a nontrivial ϕ_α^1 reads as

$$\int_{-\infty}^{\infty} -\zeta v \left(\frac{\partial \phi_\alpha^0}{\partial \eta} \right)^2 \partial \eta = \int_{-\infty}^{\infty} \frac{1}{2} [c^\alpha(\mu_{eq},T) - c^\beta(\mu_{eq},T)]$$
$$\times (\mu^0 - \mu_{eq}) \frac{\partial h_\alpha(\phi_\alpha^0)}{\partial \phi_\alpha} \frac{\partial \phi_\alpha^0}{\partial \eta} \partial \eta.$$
$$(62)$$

By making use of the integrals $\int_{-\infty}^{\infty} (\frac{\partial \phi_\alpha^0}{\partial \eta})^2 \partial \eta = \frac{1}{2}$ and $\int_{-\infty}^{\infty} \frac{\partial h_\alpha(\phi_\alpha^0)}{\partial \phi_\alpha} \partial \eta = -1$, the equation simplifies to

$$(\mu^0 - \mu_{eq}) = \frac{-\zeta v}{[c^\beta(\mu_{eq},T) - c^\alpha(\mu_{eq},T)]}.$$
$$(63)$$

This is the departure from the equilibrium chemical potential in the *sharp-interface limit*.

B. Thin-interface limit

For the thin-interface correction, we solve the chemical potential equation at the next order at $1/\epsilon$ as

$$-\left(\frac{\partial c^\alpha(\mu^0,T)}{\partial \mu} h_\alpha(\phi_\alpha^0) + \frac{\partial c^\beta(\mu^0,T)}{\partial \mu} [1 - h_\alpha(\phi_\alpha^0)] \right) \frac{v}{\epsilon} \frac{\partial \mu^0}{\partial \eta}$$
$$= \frac{1}{\epsilon} \frac{\partial}{\partial \eta} \left([1 - g_\alpha(\phi_\alpha^0)] \frac{\partial c^\beta(\mu^0,T)}{\partial \mu} \frac{\partial \mu^1}{\partial \eta} \right) + \frac{1}{\epsilon} \frac{\partial}{\partial \eta} \left(v s(\phi_\alpha^0) [c^\beta(\mu^0,T) - c^\alpha(\mu^0,T)] \frac{\partial \phi_\alpha^0}{\partial \eta} \right)$$
$$+ \frac{v}{\epsilon} [c^\alpha(\mu^0,T) - c^\beta(\mu^0,T)] \frac{\partial h_\alpha(\phi_\alpha^0)}{\partial \eta}.$$
$$(64)$$

Note that at order $1/\epsilon$, there are additional terms. However, we make use of the fact that μ^0 is constant and hence all its derivatives vanish, so that Eq. (64) simplifies to

$$\frac{\partial}{\partial \eta} \left([1 - g_\alpha(\phi_\alpha^0)] \frac{\partial c^\beta(\mu^0,T)}{\partial \mu} \frac{\partial \mu^1}{\partial \eta} \right)$$
$$= -v \frac{\partial}{\partial \eta} \left(s(\phi_\alpha^0)[c^\beta(\mu^0,T) - c^\alpha(\mu^0,T)] \frac{\partial \phi_\alpha^0}{\partial \eta} \right) + v[c^\beta(\mu^0,T) - c^\alpha(\mu^0,T)] \frac{\partial h_\alpha(\phi_\alpha^0)}{\partial \eta}.$$
$$(65)$$

By integrating this once, we get

$$\left([1 - g_\alpha(\phi_\alpha^0)] \frac{\partial c^\beta(\mu^0,T)}{\partial \mu} \frac{\partial \mu^1}{\partial \eta} \right)$$
$$= -v \left(s(\phi_\alpha^0)[c^\beta(\mu^0,T) - c^\alpha(\mu^0,T)] \frac{\partial \phi_\alpha^0}{\partial \eta} \right) + v[c^\beta(\mu^0,T) - c^\alpha(\mu^0,T)] h_\alpha(\phi_\alpha^0) + A_2.$$
$$(66)$$

To fix A_2, we take $\lim_{\eta \to -\infty}$, which gives $[1 - g_\alpha(\phi_\alpha)] \to 0$, $\frac{\partial c^\beta(\mu^0,T)}{\partial \mu}$ is a positive constant, $\frac{\partial \phi_\alpha^0}{\partial \eta} \to 0$, and $h_\alpha(\phi_\alpha^0) \to 1$. Therefore, the value of $A_2 = -v[c^\beta(\mu^0,T) - c^\alpha(\mu^0,T)]$. By substituting this in the above equation and rearranging, we get

$$\frac{\partial \mu^1}{\partial \eta} = \frac{v[c^\beta(\mu^0,T) - c^\alpha(\mu^0,T)] \left(h_\alpha(\phi_\alpha^0) - 1 - s(\phi_\alpha^0) \frac{\partial \phi_\alpha^0}{\partial \eta} \right)}{\frac{\partial c^\beta(\mu^0,T)}{\partial \mu} [1 - g_\alpha(\phi_\alpha^0)]}.$$
$$(67)$$

For brevity, we denote the expression $\frac{h_\alpha(\phi_\alpha^0) - 1 - s(\phi_\alpha^0) \frac{\partial \phi_\alpha^0}{\partial \eta}}{[1 - g_\alpha(\phi_\alpha^0)]}$ as $p(\phi_\alpha^0)$. By substituting this in the preceding equation and integrating, we get

$$\mu^1 = \overline{\mu^1} + \frac{v[c^\beta(\mu^0,T) - c^\alpha(\mu^0,T)]}{\frac{\partial c^\beta(\mu^0,T)}{\partial \mu}} \int_0^\eta p(\phi_\alpha^0) \partial \eta.$$
$$(68)$$

To obtain the integration constant $\overline{\mu^1}$, we write the phase-field equation at order ϵ^2 as

$$-\zeta v \epsilon^2 \frac{\partial \phi_\alpha^1}{\partial \eta} = \epsilon^2 \frac{\partial^2 \phi_\alpha^2}{\partial \eta^2} + \epsilon^2 \frac{16}{\pi^2} \phi_\alpha^2 + \frac{1}{2} \epsilon^2 \phi_\alpha^1 [c^\alpha(\mu_{eq},T) - c^\beta(\mu_{eq},T)](\mu^0 - \mu_{eq}) \frac{\partial^2 h_\alpha(\phi_\alpha^0)}{\partial \phi_\alpha^2}$$
$$+ \frac{1}{2} \epsilon^2 [c^\alpha(\mu_{eq},T) - c^\beta(\mu_{eq},T)] \mu^1 \frac{\partial h_\alpha(\phi_\alpha^0)}{\partial \phi_\alpha},$$

$$L\phi_\alpha^2 = -\zeta v \frac{\partial \phi_\alpha^1}{\partial \eta} - \frac{1}{2} [c^\alpha(\mu_{eq},T) - c^\beta(\mu_{eq},T)] \left[\phi_\alpha^1 (\mu^0 - \mu_{eq}) \frac{\partial^2 h_\alpha(\phi_\alpha^0)}{\partial \phi_\alpha^2} + \mu^1 \frac{\partial h_\alpha(\phi_\alpha^0)}{\partial \phi_\alpha} \right].$$
$$(69)$$

The solvability condition for a nontrivial ϕ_α^2 can be derived as

$$-\int_{-\infty}^{\infty} \zeta v \frac{\partial \phi_\alpha^1}{\partial \eta} \frac{\partial \phi_\alpha^0}{\partial \eta} \partial\eta - \int_{-\infty}^{\infty} \frac{1}{2} \phi_\alpha^1 [c^\alpha(\mu_{eq},T) - c^\beta(\mu_{eq},T)](\mu^0 - \mu_{eq}) \frac{\partial^2 h_\alpha(\phi_\alpha^0)}{\partial \phi_\alpha^2} \frac{\partial \phi_\alpha^0}{\partial \eta} \partial\eta$$

$$-\int_{-\infty}^{\infty} \frac{1}{2} [c^\alpha(\mu_{eq},T) - c^\beta(\mu_{eq},T)] \mu^1 \frac{\partial h_\alpha(\phi_\alpha^0)}{\partial \phi_\alpha} \frac{\partial \phi_\alpha^0}{\partial \eta} \partial\eta = 0. \tag{70}$$

To see the nature of the first integral, we make use of the fact that ϕ_α^1 satisfies the phase-field equation at order ϵ, which reads as

$$L\phi_\alpha^1 = -\zeta v \frac{\partial \phi_\alpha^0}{\partial \eta} - \frac{1}{2}[c^\alpha(\mu_{eq},T) - c^\beta(\mu_{eq},T)]$$
$$\times (\mu^0 - \mu_{eq}) \frac{\partial h_\alpha(\phi_\alpha^0)}{\partial \phi_\alpha}. \tag{71}$$

The phase-field profile ϕ_α^0 is part of a *sinus* curve and hence is an odd function, which implies its derivative $\frac{\partial \phi_\alpha^0}{\partial \eta}$ is even. Similarly, the interpolation function $h_\alpha(\phi_\alpha^0)$ is an odd function and hence the function $\frac{\partial h_\alpha(\phi_\alpha^0)}{\partial \phi_\alpha}$ is an *even* function. In order to realize this, we utilize the antisymmetric property of the interpolation function with respect to the $\eta = 0$ and, equivalently, where $\phi_\alpha = 1/2$:

$$h_\alpha(\phi_\alpha^0(\eta)) - \tfrac{1}{2} = \tfrac{1}{2} - h_\alpha(\phi_\alpha^0(-\eta)). \tag{72}$$

Differentiating both sides with respect to η and using the *even* property of $\frac{\partial \phi_\alpha^0}{\partial \eta}$, we derive

$$\frac{\partial h_\alpha(\phi_\alpha(\eta))}{\partial \phi_\alpha} = \frac{\partial h_\alpha(\phi_\alpha(-\eta))}{\partial \phi_\alpha}, \tag{73}$$

which proves $\frac{\partial h_\alpha(\phi_\alpha(\eta))}{\partial \phi_\alpha}$ is even. Conversely, differentiating again implies the second derivative $\frac{\partial^2 h_\alpha(\phi_\alpha(\eta))}{\partial \phi_\alpha^2}$ is odd. Using these properties, we directly find that the right-hand side of Eq. (71) is even. Combined with the fact that the operator L is of the form $\frac{\partial^2}{\partial \eta^2} + \frac{16}{\pi^2}$, which does not modify the characteristics of the right-hand side, we derive that ϕ_α^1 is even. Putting all the arguments together results in the implication that only the second integral with the term μ^1 in the solvability condition (70) does not vanish and the solvability condition simplifies to

$$\int_{-\infty}^{\infty} \frac{1}{2}[c^\alpha(\mu_{eq},T) - c^\beta(\mu_{eq},T)]\mu^1 \frac{\partial h_\alpha(\phi_\alpha^0)}{\partial \phi_\alpha} \frac{\partial \phi_\alpha^0}{\partial \eta} \partial\eta = 0. \tag{74}$$

Inserting Eq. (68) for μ^1 into the above solvability condition, we derive an equation for $\overline{\mu^1}$ given by

$$\overline{\mu^1} = \frac{v[c^\beta(\mu^0,T) - c^\alpha(\mu^0,T)]}{\frac{\partial c^\beta(\mu^0,T)}{\partial \mu}}$$
$$\times \underbrace{\int_{-\infty}^{\infty} \left[\int_0^\eta p(\phi_\alpha^0)\partial\eta \right] \frac{\partial h_\alpha(\phi_\alpha^0)}{\partial \phi_\alpha} \frac{\partial \phi_\alpha^0}{\partial \eta} \partial\eta}_{:=M}. \tag{75}$$

With the shorthand notation M we can write

$$\mu^1 = \frac{[c^\beta(\mu^0,T) - c^\alpha(\mu^0,T]}{\frac{\partial c^\beta(\mu^0,T)}{\partial \mu}} v\left(M + \int_0^\eta p(\phi_\alpha^0)\partial\eta\right). \tag{76}$$

The thin-interface limit, which denotes the macroscopic chemical potential at first order $\widetilde{\mu}_1$, can be derived by using the $\lim_{\eta \to \pm\infty}$ and the matching condition in Eq. (52) and giving

$$\lim_{\eta \to \pm\infty} \frac{\partial \mu^1}{\partial \eta} = \frac{\partial \widetilde{\mu^0}}{\partial x}\bigg|^\pm$$
$$= \frac{[c^\beta(\mu^0,T) - c^\alpha(\mu^0,T)]}{\frac{\partial c^\beta(\mu^0,T)}{\partial \mu}} vp(\phi_\alpha^0 \pm), \tag{77}$$

where $\phi_\alpha^0\pm$ denotes the value of ϕ_α^0 at the respective bulk sides. By employing the matching condition given by Eq. (49), we have

$$\widetilde{\mu^1}|^\pm = \lim_{\eta \to \pm\infty}\left(\mu^1 - \eta \frac{\partial \widetilde{\mu^0}}{\partial x}\bigg|^\pm\right)$$
$$= \frac{[c^\beta(\mu^0,T) - c^\alpha(\mu^0,T)]}{\frac{\partial c^\beta(\mu^0,T)}{\partial \mu}} v(M + F^\pm), \tag{78}$$

where we define $F|^\pm$ as

$$F^\pm = \int_0^{\pm\infty} \left[p(\phi_\alpha^0) - p(\phi_\alpha^0 \pm) \right] \partial\eta. \tag{79}$$

We realize that the limits on both sides (solid and liquid) do not match if $F^+ \neq F^-$, which gives rise to a *chemical potential jump* at the interface. To remove this jump, one must now devise a way to make the following condition true:

$$\int_0^{\infty} \left[p(\phi_\alpha^0) + 1 \right] \partial\eta = \int_0^{-\infty} p(\phi_\alpha^0) \partial\eta, \tag{80}$$

where we have made use of the fact that $\frac{\partial \phi_\alpha^0}{\partial \eta}$ is zero at $\eta \to \pm\infty$ and $h_\alpha(\phi_\alpha^0) - 1 \to 0$ at $\eta = -\infty$ and $h(\phi_\alpha^0) = 0$ at $\eta = +\infty$. We notice that these are properties directly related to our interpolation function $h_\alpha(\phi_\alpha^0)$. We intend to retrieve the same properties [implying $p(\phi_\alpha) = h(\phi_\alpha) - 1$], which is a reasonable choice, then we get $s(\phi_\alpha^0)$ as

$$s(\phi_\alpha^0) = -\frac{g_\alpha(\phi_\alpha^0)[1 - h(\phi_\alpha^0)]}{\frac{\partial \phi_\alpha^0}{\partial \eta}}. \tag{81}$$

With this modification, we define $F := F^+(= F^-)$ and the macroscopic chemical potential $\widetilde{\mu_1}$ at first order in Eq. (78) yields

$$
\begin{aligned}
\widetilde{\mu^1}|^{\pm} &= \lim_{\eta \to \pm\infty} \left(\mu^1 - \eta \frac{\partial \widetilde{\mu^0}}{\partial x} \Big|^{\pm} \right) \\
&= \frac{[c^{\beta}(\mu^0,T) - c^{\alpha}(\mu^0,T)]}{\frac{\partial c^{\beta}(\mu^0,T)}{\partial \mu}} v(M + F) \quad (82)
\end{aligned}
$$

and the chemical potential until the first order in ϵ writes $\widetilde{\mu}|^{\pm} = \mu^0 + \epsilon \widetilde{\mu^1}|^{\pm}$, which upon subtracting μ_{eq} from both sides becomes

$$
\begin{aligned}
\widetilde{\mu}|^{\pm} &- \mu_{eq} \\
&= (\mu^0 - \mu_{eq}) + \epsilon \frac{[c^{\beta}(\mu^0,T) - c^{\alpha}(\mu^0,T)]}{\frac{\partial c^{\beta}(\mu^0,T)}{\partial \mu}} v(M + F).
\end{aligned}
$$
$$(83)$$

Putting all physical properties in their respective dimensions, we get

$$
\begin{aligned}
\widetilde{\mu}|^{\pm} &- \mu_{eq} \\
&= (\mu^0 - \mu_{eq}) + \epsilon \frac{[c^{\beta}(\mu^0,T) - c^{\alpha}(\mu^0,T)]}{(D^{\beta})\frac{\partial c^{\beta}(\mu^0,T)}{\partial \mu}} V(M + F).
\end{aligned}
$$
$$(84)$$

C. Kinetic coefficient $\overline{\beta}$ and the antitrapping current

To relate the total departure from equilibrium at first order in ϵ given in Eq. (84), it is customary to write the modified temperature of the interface T due to the Gibbs-Thomson effect written as

$$
T = T_m - |m_{\beta}|c_i^{\beta} - \Gamma\kappa - \overline{\beta}V, \quad (85)
$$

where T and c_i^{β} are the interfacial temperatures and the concentrations of the liquid, while m_{β} is the slope of the liquidus and T_m is the melting point of the pure component. $\overline{\beta}$ is the kinetic coefficient and Γ is the Gibbs-Thomson coefficient. Then, T can be written as follows:

$$
T = T_m - |m_{\beta}|c^{\beta}(\mu_{eq},T). \quad (86)
$$

With this, the Gibbs-Thompson equation is modified as

$$
(T_m - |m_{\beta}|c_i^{\beta}) - [T_m - |m_{\beta}|c^{\beta}(\mu_{eq},T)] = \Gamma\kappa + \overline{\beta}V. \quad (87)
$$

The first bracketed term on the left-hand side is the modified melting point of the interface due to constitutional undercooling because of the shift of interfacial concentration c_i^{β} with respect to the equilibrium liquidus concentration at this temperature $c^{\beta}(\mu_{eq},T)$. The second bracketed term is the temperature of solidification. Their difference is nothing but the equivalent undercooling ΔT, which matches the Gibbs-Thomson equation of a pure material. Since we are here treating only one-dimensional problems, curvature undercooling drops out and the effective undercooling reads as

$$
\Delta T = m_{\beta}[c^{\beta}(\mu_{eq},T) - c_i] = \overline{\beta}V. \quad (88)
$$

In order to relate the undercooling at the interface $\widetilde{\Delta T}$, which is the macroscopic undercooling at first order, to the deviation of the macroscopic chemical potential from equilibrium in the thin-interface limit, we multiply Eq. (84) by $m_{\beta}\frac{\partial c^{\beta}(\mu_{eq},T)}{\partial \mu}$ such that the left-hand side of the equation is nothing but $m_{\beta}[c_i^{\beta} - c^{\beta}(\mu_{eq},T)]$and, alternatively, $-\widetilde{\Delta T}$. With this modification, the total Eq. (84) becomes

$$
-\widetilde{\Delta T}|^{\pm} = m_{\beta}\frac{\partial c^{\beta}(\mu_{eq},T)}{\partial \mu}\left[(\mu^0 - \mu_{eq}) + \epsilon \frac{[c^{\beta}(\mu^0,T) - c^{\alpha}(\mu^0,T)]}{(D^{\beta})\frac{\partial c^{\beta}(\mu^0,T)}{\partial \mu}} V(M + F) \right]. \quad (89)
$$

Using the result obtained in Eq. (63), inserting the appropriate dimensions, and substituting the relation between the undercooling and the kinetic coefficient ($\widetilde{\Delta T}|^{\pm} = \widetilde{\overline{\beta}}|^{\pm}V$), we derive the equation of the kinetic coefficient ($\widetilde{\overline{\beta}}|^{\pm} = \widetilde{\overline{\beta}}$) as

$$
\widetilde{\overline{\beta}} = \frac{m_{\beta}\frac{\partial c^{\beta}(\mu_{eq},T)}{\partial \mu}}{[c^{\beta}(\mu_{eq},T) - c^{\alpha}(\mu_{eq},T)]}\left[\omega - \epsilon \frac{[c^{\beta}(\mu^0,T) - c^{\alpha}(\mu^0,T)][c^{\beta}(\mu_{eq},T) - c^{\alpha}(\mu_{eq},T)]}{(D^{\beta})\frac{\partial c^{\beta}(\mu^0,T)}{\partial \mu}} (M + F) \right]. \quad (90)
$$

Now, we make the approximation $[c^{\beta}(\mu^0,T) - c^{\alpha}(\mu^0,T)] \approx [c^{\beta}(\mu_{eq},T) - c^{\alpha}(\mu_{eq},T)]$, which is valid for small driving forces. Utilizing the approximation, the expression for the kinetic coefficient until the first order becomes

$$
\widetilde{\overline{\beta}} = \frac{m_{\beta}\frac{\partial c^{\beta}(\mu_{eq},T)}{\partial \mu}}{[c^{\beta}(\mu_{eq},T) - c^{\alpha}(\mu_{eq},T)]}\left[\omega - \epsilon \frac{[c^{\beta}(\mu_{eq},T) - c^{\alpha}(\mu_{eq},T)]^2}{(D^{\beta})\frac{\partial c^{\beta}(\mu^0,T)}{\partial \mu}} (M + F) \right]. \quad (91)
$$

An alternative form can also be written using some basic thermodynamics relating $\frac{\partial c^\beta(\mu_{eq},T)}{\partial\mu}$ with the latent heat of transformation L^α using the Clausius-Clapeyron equation for alloys, which writes as $\frac{d\mu_{eq}}{dT} = \frac{\partial\mu_{eq}}{\partial c^\beta}\frac{dc^\beta(\mu_{eq},T)}{dT} = \frac{L^\alpha}{T[c^\beta(\mu_{eq},T)-c^\alpha(\mu_{eq},T)]}$. By using $m_\beta = \frac{dc^\beta(\mu_{eq},T)}{dT}$, we derive $\frac{m_\beta\frac{\partial c^\beta(\mu_{eq},T)}{\partial\mu}}{[c^\beta(\mu_{eq},T)-c^\alpha(\mu_{eq},T)]} = \frac{T}{L^\alpha}$. This gives an equivalent form for the kinetic coefficient as

$$\widetilde{\overline{\beta}} = \frac{T}{L^\alpha}\left[\omega - \epsilon\frac{[c^\beta(\mu_{eq},T)-c^\alpha(\mu_{eq},T)]^2}{(D^\beta)\frac{\partial c^\beta(\mu^0,T)}{\partial\mu}}(M+F)\right]. \tag{92}$$

From this, it is easy to see that to perform simulations with vanishing interface kinetic coefficient ($\widetilde{\overline{\beta}} = 0$), one can choose the relaxation constant ω according to the relation

$$\omega = \epsilon\frac{[c^\beta(\mu_{eq},T)-c^\alpha(\mu_{eq},T)]^2}{(D^\beta)\frac{\partial c^\beta(\mu^0,T)}{\partial\mu}}(M+F). \tag{93}$$

For the typical interpolation polynomials of cubic and quartic type polynomial, when used in combination with the obstacle potential, the values of F and M are tabulated below:

	M	F
$h(\phi_\alpha) = \phi_\alpha^2(3-2\phi_\alpha)$	0.063828	0.158741
$h(\phi_\alpha) = \phi_\alpha^3(10-15\phi_\alpha+6\phi_\alpha^2)$	0.052935	0.129288

Finally, the antitrapping current along with the derived $s(\phi_\alpha^0)$ in Eq. (81) is given by

$$j_{at} = -\frac{\pi\epsilon}{4}\frac{g_\alpha(\phi_\alpha^0)[1-h_\alpha(\phi_\alpha^0)]}{\sqrt{\phi_\alpha^0(1-\phi_\alpha^0)}}$$
$$\times[c^\beta(\mu^0,T)-c^\alpha(\mu^0,T)]\frac{\partial\phi_\alpha}{\partial t}\frac{\nabla\phi_\alpha}{|\nabla\phi_\alpha|}. \tag{94}$$

D. Effect of curvature and anisotropy

With the above analysis, we derive the expressions for the relaxation constant and the antitrapping current, which are dependent on the chemical potential at the zeroth order μ^0. While in one-dimensional problems its value depends on the local normal velocity and can be determined by Eq. (63), in the presence of curvature, the Gibbs-Thomson condition is modified through the contribution of the term proportional to $\sigma\kappa$, which modifies the sharp-interface limit for isotropic surface energies, given in Eq. (63) in dimensional units as

$$(\mu^0 - \mu_{eq}) = \frac{\omega V}{[c^\alpha(\mu_{eq},T)-c^\beta(\mu_{eq},T)]}$$
$$+ \frac{\sigma\kappa}{c^\alpha(\mu_{eq},T)-c^\beta(\mu_{eq},T)}. \tag{}$$

The preceding equation can be derived by considering the extra term arising from writing the Laplacian in curvilinear coordinates represented using the curvature κ and the arc length as in [6,14]. The value of the chemical potential μ^0 derived through the preceding expression is difficult to utilize in the expressions derived for the kinetic coefficient

and the antitrapping current since the values of the curvature and the velocity are not known *a priori*. A workaround for this problem would be to use the approximation $\frac{\partial c^\beta(\mu^0,T)}{\partial\mu} \approx \frac{\partial c^\beta(\mu_{eq},T)}{\partial\mu}$, which is valid for small departures from equilibrium relevant for most phase transition problems occurring at lower undercoolings in the absence of appreciable interface kinetics. The same approximation can also be applied for the rejection $c^\alpha(\mu^0,T) - c^\beta(\mu^0,T)$ appearing in both the expressions for the relaxation constant and the antitrapping current, which varies little from its value at at the equilibrium chemical potential for lower undercoolings.

For larger departures from equilibrium, we propose to dynamically evaluate the expressions for the relaxation constant ω and the antitrapping current. To do this, we need the chemical potential in the sharp-interface limit, which is the average value across the interface. Since this is computationally time consuming to evaluate, we use the local chemical potential for the dynamic computation of the above mentioned quantities. This introduces an error of order $O(\epsilon^2)$ and higher for the antitrapping, which can be realized by expanding the term $c^\beta(\mu^0,T) - c^\alpha(\mu^0,T)$ around the local chemical potential μ. The highest order correction would be proportional to $(\frac{\partial c^\beta}{\partial\mu} - \frac{\partial c^\alpha}{\partial\mu})(\mu^0 - \mu)$, where $\mu^0 - \mu$ is at highest order proportional to $O(\epsilon)$ rendering the leading order correction due to this implementation of the antitrapping current proportional to $O(\epsilon^2)$. A similar result can be derived for the case of the relaxation constant ω. Since, in the thin-interface limit, we only claim to derive the relations with accuracy of order $O(\epsilon)$, this scheme should be certainly acceptable.

Another point worth mentioning concerns the treatment of anisotropy in kinetics. While using Eq. (93), problems with vanishing interface kinetics in isotropic situations can be treated in order to achieve interface evolution with nonvanishing interface kinetics in the case of isotropic system, which would require the back calculation of the relaxation constant through Eq. (92). The more realistic situation of anisotropy in surface energy and kinetics can be treated through a modification of Eq. (93). We follow a route suggested in [14,15] of a simple derivation by writing the equations of motion for the normal direction, but excluding curvature. The anisotropy in the surface energy is affected by writing the gradient energy contribution as $\gamma_0 a_c(\mathbf{n})^2|q_{\alpha\beta}|^2$, where $\mathbf{n}$ is the unit normal vector to the interface defined as $\frac{q_{\alpha\beta}}{|q_{\alpha\beta}|}$ and $a_c(\mathbf{n})$ describes the anisotropy in the surface energy. A similar function $\omega(\mathbf{n})$ is used for tailoring the anisotropy in the kinetic coefficient. The major modification in the asymptotics through this calculation is the transformation of the gradient in the phase-field profile at leading order, which becomes $\frac{\partial\phi_\alpha^0}{\partial\eta} = -\frac{1}{a_c(\mathbf{n})}\frac{4}{\pi}\sqrt{\phi_\alpha^0(1-\phi_\alpha^0)}$. Incorporating this result in the asymptotics yields the following expression for the kinetic coefficient:

$$\widetilde{\overline{\beta}}(\mathbf{n}) = \frac{T}{L^\alpha}\left[\frac{\omega(\mathbf{n})}{a_c(\mathbf{n})} - \epsilon a_c(\mathbf{n})\right.$$
$$\left.\times\frac{[c^\beta(\mu_{eq},T)-c^\alpha(\mu_{eq},T)]^2}{(D^\beta)\frac{\partial c^\beta(\mu^0,T)}{\partial\mu}}(M+F)\right]. \tag{95}$$

To achieve vanishing interface kinetics in all directions, we can choose $\omega(\mathbf{n})$ as $\omega_0 a_c(\mathbf{n})^2$, where ω_0 is derived from the expression in Eq. (93). The case of anisotropy in kinetics would, however, require a more careful evaluation of the functions. Lastly, we would like to recall that a linearization of the grand potential around the equilibrium chemical potential was used for deriving the asymptotics. This is valid for small departures from equilibrium in phase transitions occurring at low undercoolings, where interface kinetics is absent and small. For certain situations at very high undercoolings and in the presence of strong kinetics, there might arise a situation where this linearization does not hold. This depends on the nature of the grand potentials and the magnitude of departure from equilibrium. The linearization is, however, only a simplification that can be easily relaxed resulting in the modification of the sharp-interface limit for isotropic surface energies through the relation

$$\Psi_\beta(\mu^0,T) - \Psi_\alpha(\mu^0,T) = \sigma\kappa + \omega V. \quad (96)$$

The derivation of the deviation of the chemical potential, however, depends on the nature of the grand potentials, where expansions of the grand potentials, until first or second order in the term $\mu^0 - \mu_{eq}$, might be necessary. The expression for the chemical potential at first order remains unchanged. However, no general rule exists for estimating the validity of the linearization used in the asymptotics, and the departure from equilibrium must be used to estimate the difference between the linearized and the original grand-potential descriptions before reaching a conclusion.

From the above discussion, we have all the corrections that we need for performing quantitative simulations. The corrections to the Stefan condition at higher orders, which are the *interface stretching* and the *surface diffusion*, vanish when antisymmetric functions are used to interpolate the phase diffusivities $g_\alpha(\phi_\alpha)$ and $h_\alpha(\phi_\alpha)$ for the grand potentials that are applied from results derived in previous literature [6,11]. In the next section, we perform test benchmarks to quantitatively evaluate the effect of the calculations.

III. BENCHMARK

To benchmark our calculations, we construct a system to model the Al-Cu system on the Al-rich side and we denote the concentration of the single independent component Al as $c = c_{Al}$. The free energies for the α and the liquid are chosen in the following manner:

$$f^\alpha(T,c) = f^* \left(c L_{Al}^\alpha \frac{(T - T_{Al}^\alpha)}{T_{Al}^\alpha} + (1-c) L_{Cu}^\alpha \frac{(T - T_{Cu}^\alpha)}{T_{Cu}^\alpha} \right.$$
$$\left. + T[c \ln c + (1-c)\ln(1-c)] \right), \quad (97)$$

$$f^l(T,c) = f^* \{ T[c \ln c + (1-c)\ln(1-c)] \}.$$

From these expressions, the chemical potentials μ^α and μ^l can be derived as

$$\mu^\alpha = f^* \left[L_{Al}^\alpha \frac{(T - T_{Al}^\alpha)}{T_{Al}^\alpha} - L_{Cu}^\alpha \frac{(T - T_{Cu}^\alpha)}{T_{Cu}^\alpha} \right.$$
$$\left. + T \ln\left(\frac{c^\alpha}{1-c^\alpha}\right) \right], \quad (98)$$

$$\mu^l = f^* \left[T \ln\left(\frac{c^l}{1-c^l}\right) \right]. \quad (99)$$

Using these expressions, the information of the free energy versus composition can be transformed into functions $c^\alpha(\mu,T)$ and $c^l(\mu,T)$ for each phase by inverting the above expressions for the chemical potential as

$$c^\alpha(\mu,T) = \frac{\exp\left[\frac{\mu - (L_{Al}^\alpha \frac{(T-T_{Al}^\alpha)}{T_{Al}^\alpha} - L_{Cu}^\alpha \frac{(T-T_{Cu}^\alpha)}{T_{Cu}^\alpha})}{f^* T}\right]}{1 + \exp\left[\frac{\mu - (L_{Al}^\alpha \frac{(T-T_{Al}^\alpha)}{T_{Al}^\alpha} - L_{Cu}^\alpha \frac{(T-T_{Cu}^\alpha)}{T_{Cu}^\alpha})}{f^* T}\right]}, \quad (100)$$

$$c^l(\mu,T) = \frac{\exp\left[\frac{\mu}{f^* T}\right]}{1 + \exp\left[\frac{\mu}{f^* T}\right]}. \quad (101)$$

Notice that we have written $c^\alpha(\mu,T)$ and $c^l(\mu,T)$ as functions of a unique μ as required by the grand-potential formulation. The parameters of the free energy densities have been chosen in a manner such that we have the Gibbs-Thomson coefficient set to the value 2.4×10^{-7} K/m, which is reported in literature [16]. The solid-liquid surface energy is chosen as 0.35 J/m^2, which is an average value for metallic systems. Consistent with the above quantities, the energy density scale f^* is derived as 73.5×10^{-7} J/m^3. We fit the slopes of the liquidus and the concentrations of the solid and liquid at 870 K. Next, we nondimensionalize the whole set of evolution equations using the energy scale as f^*, the length scale $d_o = \sigma_{\alpha\beta}/f^*$, and the time scale as $t^* = d_o^2/D^l$, and the reference temperature is melting point of pure aluminium. The phase diagram corresponding to these parameters is plotted in Fig. 3. The simulation parameters with this scaling are $L_{Cu}^\alpha = 8.45$ and $L_{Al}^\alpha = 5.30$, while $T_{Cu}^\alpha = 0.422\,73$ and $T_{Al}^\alpha = 1.0$. The kinetic coefficient can be computed both for finite and infinite phase-field interface mobility. For our computations, we set the infinite interface kinetics in all directions. Our simulations are performed with smooth cubic anisotropy of the form

$$a_c(q_{\alpha\beta}) = 1 - \delta_{\alpha\beta}\left(3 - 4\frac{|q_{\alpha\beta}|_4^4}{|q_{\alpha\beta}|^4}\right), \quad (102)$$

where $|q_{\alpha\beta}|_4^4 = \sum_i^d (q_{\alpha\beta})_i^4$ and $|q_{\alpha\beta}|^4 = [\sum_{i=1}^d (q_{\alpha\beta})_i^2]^2$, d being the number of dimensions. $\delta_{\alpha\beta}$ is the strength of the
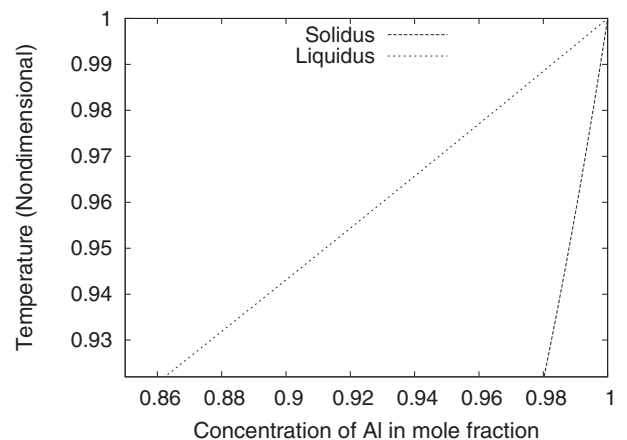

FIG. 3. The phase diagram of the Al-Cu system fitted on the Al-rich side using an ideal solution type of model.
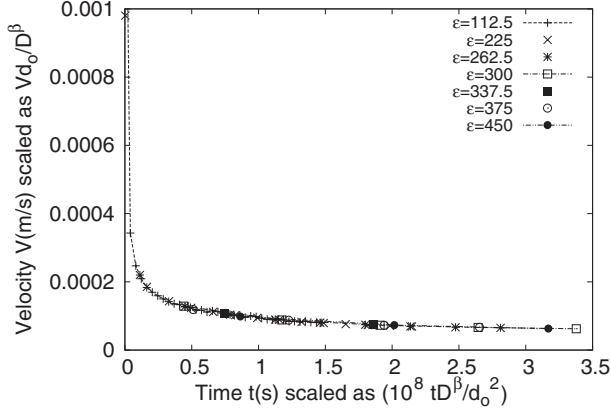
FIG. 4. Plot of the dendrite tip velocities simulated at a temperature of $T = 0.9843$. We selectively plot points corresponding to a simulation to show the convergence of the velocities. We span a range where ϵ varies by a factor 4 and achieve convergence in the velocities. The simulation with the $\epsilon = 112.5$ has run the least in nondimensional time (1.5×10^8), but long enough to confirm convergence of the velocities.

anisotropy, which is set to 0.0097 for the chosen alloy of Al 4 wt% Cu [17]. To have vanishing interface kinetics in all directions, we employ the same strategy as [14,15] by choosing the form of the relaxation constant as a function of the normal vector $q_{\alpha\beta}$ given by

$$\omega(q_{\alpha\beta}) = \omega_0 a_c^2(q_{\alpha\beta}), \tag{103}$$

where ω_0 is computed using the relation in Eq. (93).

The simulation setup involves a free dendrite growing into a uniformly undercooled melt. Utilizing the symmetry of the surface energy anisotropy, we simulate one quadrant of the dendrite. The first benchmark involves the proof of invariance of the dendrite tip velocities with varying
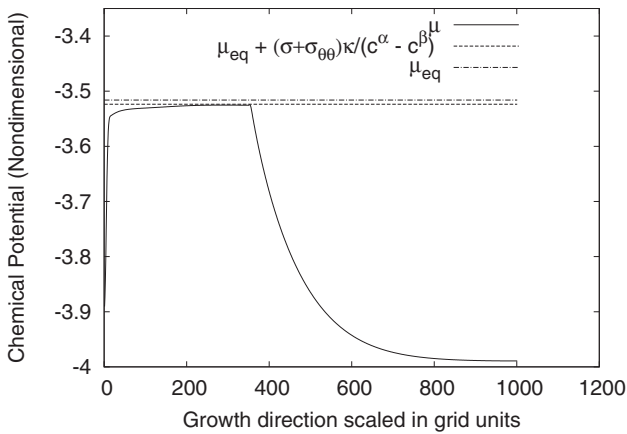

FIG. 5. Chemical potential plot along a linear section at the dendrite tip in the growing direction, superimposed with the lines showing the equilibrium chemical potential and the theoretically predicted chemical potential obtained by considering the shift because of Gibbs-Thomson effect due to curvature. The curvature used in the calculation is measured at the dendrite tip from the simulation. $\sigma_{\theta\theta}$ represent the second derivative of the surface tension as a function of the polar angle, and the sum $\sigma + \sigma_{\theta\theta}$ represents the stiffness of the interface.

interface widths. For this, we set the nondimensional bulk temperature at $T = 0.9843$ where the melting temperature of the chosen alloy composition Al 1.732 at.% is $T = 0.99$. Figure 4 plots the dendrite tip velocities upon change in the interface widths, which confirms our calculations that there exists a range in interface widths for which the interface velocities are invariant. Above the maximum considered ϵ, the interface becomes unstable and the asymptotics seems to break down and we suppose this occurs because errors of order $O(\epsilon^2)$ become appreciable. Figure 5 displays the chemical potential along a linear section at the dendrite tip in the growing direction, along with the equilibrium chemical potential and the theoretical chemical potential derived from the Gibbs-Thomson condition considering only the effect of curvature. The results show good agreement, confirming the asymptotic expressions and the developed model. The contours of the chemical potential and the phase profiles in a section of the domain showing the growing dendrite is portrayed in Fig. 6.

A. Free energy functional versus grand-potential functional

In this section, we present a short discussion on the range of applicability of the models derived from the grand-potential and the free energy functional. The comparison is with respect to the computational efficiency in simulating a range of undercoolings for both models and the asymptotics. To start with, we write the evolution equation for the phase-field variables for a system of two phases and two components, starting from the free energy functional

$$\omega\epsilon \frac{\partial \phi_\alpha}{\partial t} = \gamma_{\alpha\beta}\epsilon \frac{\partial^2 \phi_\alpha}{\partial x^2} - \frac{\gamma_{\alpha\beta}}{\epsilon}\frac{16}{2\pi^2}(1 - 2\phi_\alpha)$$
$$- \frac{1}{2}\frac{df}{d\phi_\alpha} + \frac{1}{2}\frac{\partial f}{\partial c}\frac{dc}{d\phi_\alpha}.$$

Noting that for this formulation based on the free energy functional $\mu = \frac{\partial f}{\partial c}$, the equation can be manipulated as

$$\omega\epsilon^2 \frac{\partial \phi_\alpha}{\partial t} = \gamma_{\alpha\beta}\epsilon^2 \frac{\partial^2 \phi_\alpha}{\partial x^2}$$
$$- \left\{ \gamma_{\alpha\beta}\frac{16}{2\pi^2}(1 - 2\phi_\alpha) + \frac{\epsilon}{2}\frac{d}{d\phi_\alpha}(f - \mu_{eq}c) \right\}$$
$$+ \frac{\epsilon}{2}(\mu - \mu_{eq})\frac{dc}{d\phi_\alpha}.$$

At equilibrium $\mu = \mu_{eq}$, the second bracketed term has the form of a potential and when $\epsilon f^* \approx \gamma_{\alpha\beta}$, where f^* is the energy scale, the potential scales with the length scale of the interface scales with ϵ. In the sharp-interface limit, the chemical potential at the leading order is constant across the interface, rendering sharp interface limit for one-dimensional evolution, as derived in Eq. (11). We would derive a similar sharp-interface limit with the grand-potential functional in the absence of curvature. Note, however, that the effective potential in the case of the free energy functional scales with the interface width. This contribution leads to the modification of the surface energies and, hence, in the presence of curvature, the limits will differ. Additionally, there is a deviation in the phase-field profile at leading order, which is modified due to

the presence of the grand-potential excess as

$$\frac{\partial \phi_\alpha}{\partial x} = -\frac{1}{\epsilon}\sqrt{\frac{16}{\pi^2}\phi_\alpha(1-\phi_\alpha) + \frac{\epsilon}{\gamma_{\alpha\beta}}[(f-\mu_{eq}c)-(f-\mu_{eq}c)_{\text{bulk}}]} \tag{104}$$

in contrast to $\frac{\partial \phi_\alpha}{\partial x} = -\frac{4}{\epsilon\pi}\sqrt{\phi_\alpha(1-\phi_\alpha)}$ for the case of the grand-potential functional. This modifies the effective kinetic coefficient applicable for both models. Therefore, to perform comparative simulations with the two models, the first challenge is to set the surface energies at leading order in the two models equivalent. The next is to derive the desired interface width to perform efficient simulations and finally to set the same kinetic coefficients for both models.

While in the case of the grand-potential functional the interface width depends directly on the parameter ϵ, through the relation $\frac{\pi^2\epsilon}{4} = 2.5\epsilon$, and the surface energy is the same as the simulation parameter $\gamma_{\alpha\beta}$, for the case of the free energy functional an expression for the interface width and surface energy at leading order can be derived as in Eqs. (4), and (5). By solving these equations simultaneously, we can derive

the simulation parameters $\gamma_{\alpha\beta}$ and ϵ to derive the surface energies $\sigma_{\alpha\beta}$ and $\Lambda_{\alpha\beta}$ for the given free energy functional. Whereas, this is possible for certain choices of ϵ, such as displayed in Fig. 7(a), beyond a critical ϵ there exists no unique solution when the contribution to the potential from the grand-potential excess becomes dominant over that from the potential term $\gamma_{\alpha\beta}\phi_\alpha(1-\phi_\alpha)$. The solution is then achieved for a range of $\gamma_{\alpha\beta}$ and ϵ derived through the overlap of the isolevels of the $\sigma_{\alpha\beta}$ and the resulting $\lambda_{\alpha\beta}$, which is fixed upon choosing the isolevel for the surface energy [Fig. 7(b)]. The computational efforts can be compared between the two models by estimating the interface widths used when the same ϵ is chosen for both the models. At the temperature $T = 0.988$, Fig. 8 displays the contours of a freely growing dendrite at a temperature of $T = 0.988$ ($T_m = 0.99$) simulated using the
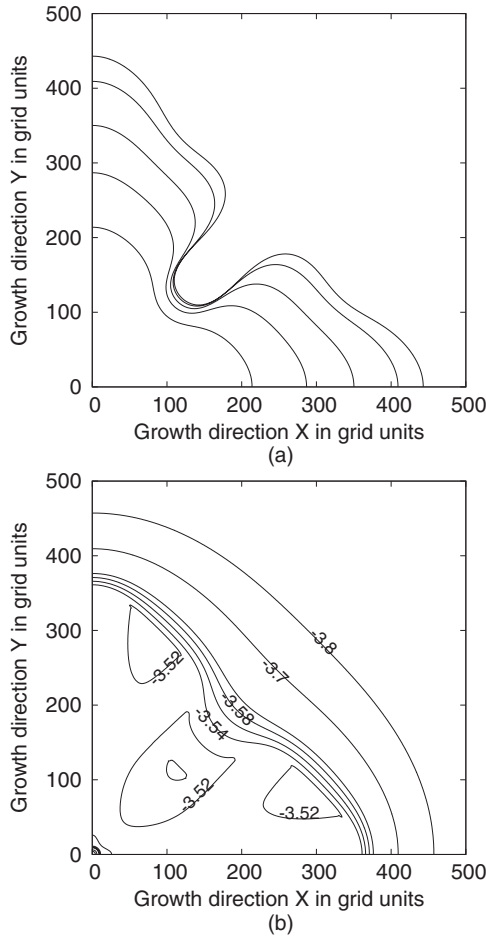

FIG. 6. Isolevel $\phi_\alpha = 0.5$ denoting the binary interface between the solid and the liquid at various times is shown in (a), while the contours of the chemical potential at a particular instant during evolution is displayed in (b). Values of some of the contours of the respective nondimensionalized chemical potential are superimposed on the plot. The simulations correspond to the case when $\epsilon = 300$.
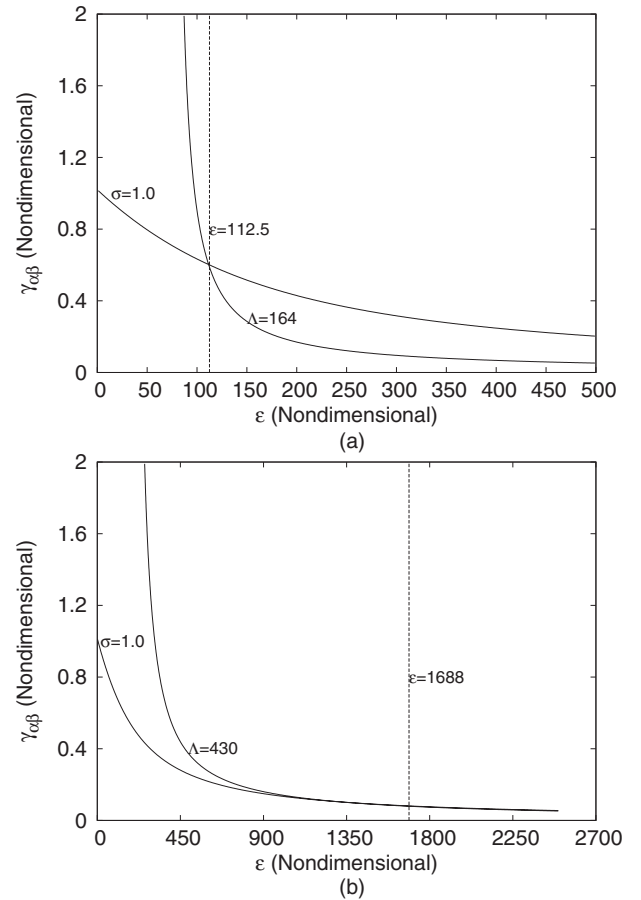

FIG. 7. Defined contour level of the surface energy σ and the interface width λ plotted as a function of the simulation parameters $\gamma_{\alpha\beta}$ and ϵ. In (a), the contours are calculated for the temperature $T = 0.9843$, while in (b) they are for a temperature of $T = 0.988$. The contours of the interface width are calculated from the defined level for the surface energy and the value of the ϵ used in the simulation. All terms are dimensionless in the graphs.
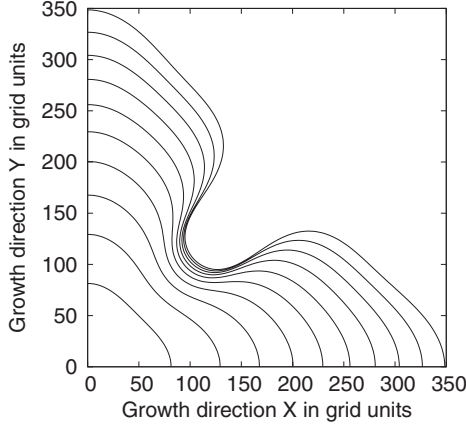
FIG. 8. Phase-field contours of a free growing equiaxed dendrite, with $\epsilon = 1688$ at a temperature of $T = 0.988$ ($T_m = 0.99$) with the grand-potential formulation.
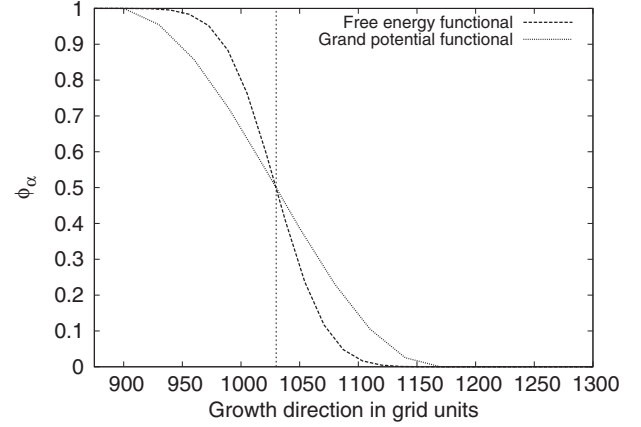

FIG. 9. Comparison of the leading order solution of the phase field in the case of the grand-potential functional and the free energy functional. The profiles have been superimposed, and the vertical line representing the position of the binary interface is drawn for comparison.

grand-potential formulation with $\epsilon = 1688$. Corresponding to this ϵ, the interface width is $\lambda = 430$ for the case of the free energy functional [Fig. 7(b)]. To have an interface resolution of 10 cells would result in a grid resolution of $\Delta x = 43$ when simulations are performed using a regular grid. In contrast, for the case with a grand-potential functional, we have used $\Delta x = 500$ for the simulation of the dendrite displayed in Fig. 8, keeping the same interface resolution and conditions, which implies the computational effort increases 10^d times (d denoting the dimension), when using the free energy functional. The situation is more favorable for the free energy functional at the higher undercooling at $T = 0.9843$ (smaller tip radii), as can be seen from Fig. 7(a), where the interface width for the free energy case results in 164 compared to a value of 281.5 for the grand-potential functional at the same $\epsilon = 112.5$. This is, however, not the largest interface width that can be employed at this undercooling, and much larger interface widths can be used for the case of the grand-potential functional as was seen in Fig. 4, while the interface widths that can be employed, when a free energy functional is used, gets limited to a smaller range. In summary, we conclude that at higher undercoolings (finer microstructures), the models based on the free energy functional and the grand-potential functionals come closer. However, at lower velocities or at lower undercoolings, the grid resolution can be scaled up significantly using the grand-potential functional, which is, however, not a possibility using the free energy functional.

The comparison of the two models is incomplete without the discussion on the interface kinetics. As we have derived, larger interface widths can be employed for simulating the case of lower undercoolings with the grand-potential functional. For such cases, the thin-interface limit is appropriate, and in this limit, the parameters can be chosen in such a manner that interface kinetics vanishes, which is relevant at lower undercoolings. To perform a similar asymptotics for the free energy functional seems daunting and less useful because of the following reasoning. We recall that while performing the thin-interface asymptotics of the grand-potential functional, we have repeatedly used the antisymmetric properties (odd functions) of the leading order phase-field profile $\phi_\alpha^0(x)$, which reduced the terms contributing to the first order correction

to the chemical potential. However, with the free energy functional, the leading order solution is modified due to the grand-potential excess and is derived using Eq. (104). Figure 9 compares the profiles in both cases, which show slight asymmetry about the $\phi_\alpha = 0.5$ line in the case of the free energy functional. The magnitude of the asymmetry depends on the nature of the grand-potential excess and scales with the interface widths. This asymmetry would rule out any general simplification of the solvability integrals appearing in the asymptotic analysis. Second, all solvability integrals depend on the leading order solution, which change with the interface widths the temperature and the system one is simulating, thus certainly hindering the universal applicability of the analysis. Lastly, due to the limitation of the interface widths, the thin-interface limit is less applicable, and performing simulations with vanishing interface kinetics is computationally expensive as the sharp-interface and thin-interface limits coincide for smaller interface widths.

To conclude, the grand-potential formulation offers significant flexibility in comparison to the free energy functionals because the range of applicability of the phase-field models is improved significantly without a corresponding increase in computational overhead, and additionally, a thin-interface asymptotics with universal applicability can be performed.

IV. CONCLUSIONS

We present a multi-phase-field model based on the grand-potential functional. This modification enables us to effectively decouple the bulk and interface contributions, which in turn allows us to upscale the length of simulations. This formulation is consistent with existing quantitative phase-field models and places it in a common framework starting from a grand-potential functional. We perform an asymptotic analysis of the derived model and obtain the thin-interface limit for the kinetic coefficient and an expression for the antitrapping current for the special case of *double-obstacle-type* potentials. It is noteworthy to mention that, computationally, the obstacle-type potentials are more efficient because the interface is finitely

defined. Hence, computations of the gradient terms can be finitely limited to a fixed number of points in the interface. This computational efficiency was offset until now because there was no existing thin-interface limit and no expressions for the antitrapping current for these types of potentials. This precluded the possibility of performing any quantitative simulations for the case of alloys. However, with the present thin-interface asymptotics, this can now be realized. One must also note that although this study has been performed for the case of two-phase alloy solidification, this is not a limitation and the analysis can be easily generalized similar to earlier works [6]. For example, the antitrapping current for the case of multiphase, multicomponent alloy solidification, where all the solid phases have zero diffusivities, can be obtained by averaging each of the individual fluxes for each component i given by

$$
\left(j_{at}^{\alpha \to l}\right)_i = -\frac{\pi \epsilon}{4} \frac{g_\alpha\left(\phi_\alpha^0\right)\left[1 - h_\alpha\left(\phi_\alpha^0\right)\right]}{\sqrt{\phi_\alpha^0\left(1 - \phi_\alpha^0\right)}}
$$
$$
\times \left[c_i^\beta(\mu) - c_i^\alpha(\mu)\right] \frac{\partial \phi_\alpha}{\partial t} \frac{\nabla \phi_\alpha}{|\nabla \phi_\alpha|}, \qquad (105)
$$

and summing up all the fluxes projected along the normal to the liquid phase-field contour as

$$
(j_{at})_i = \sum_{\alpha=1}^{N} \left(j_{at}^{\alpha \to l}\right)_i \left(-\frac{\nabla \phi_\alpha}{|\nabla \phi_\alpha|} \cdot \frac{\nabla \phi_l}{|\nabla \phi_l|}\right). \qquad (106)
$$

Other possibilities also exist, and the generalized normal vector $q_{\alpha l}$ can itself be used for the projection. Similarly, the relaxation constant for a vanishing interface coefficient for more than two components can be obtained similar to [13], which is an extension of our present analysis. With such modifications, quantitative simulations of multiphase, multicomponent systems at larger scales have become computationally feasible.

[1] V. D. Waals, Z. Phys. Chem. **13**, 657 (1894).

[2] H. Garcke, B. Nestler, and B. Stinner, SIAM J. Appl. Math. **64**, 775 (2004).

[3] B. Nestler, H. Garcke, and B. Stinner, Phys. Rev. E **71**, 041609 (2005).

[4] S. G. Kim, W. T. Kim, and T. Suzuki, Phys. Rev. E **58**, 3316 (1998).

[5] P. R. Cha, D. H. Yeon, and J. K. Yoon, Acta Mater. **49**, 3925 (2001).

[6] B. Echebarria, R. Folch, A. Karma, and M. Plapp, Phys. Rev. E **70**, 061604 (2004).

[7] J. Tiaden, B. Nestler, H. J. Deipers, and I. Steinbach, Phys. D (Amsterdam) **115**, 73 (1998).

[8] J. Eiken, B. Böttger, and I. Steinbach, Phys. Rev. E **73**, 066122 (2006).

[9] A. A. Wheeler, W. J. Boettinger, and G. B. McFadden, Phys. Rev. A **45**, 7424 (1992).

[10] M. Plapp, Phys. Rev. E **84**, 031601 (2011).

[11] A. Karma, Phys. Rev. Lett. **87**, 115701 (2001).

[12] R. F. Almgren, SIAM J. Appl. Math **59**, 2086 (1999).

[13] S. G. Kim, Acta Mater. **55**, 4391 (2007).

[14] A. Karma and W. J. Rappel, Phys. Rev. E **57**, 4323 (1998).

[15] A. Karma and W. J. Rappel, Phys. Rev. E **53**, R3017 (1996).

[16] M. Gunduz and J. D. Hunt, Acta Metall. **33**, 1651 (1985).

[17] S. Liu, R. E. Napolitano, and R. Trivedi, Acta Mater. **49**, 4271 (2001).